Electric Power Systems Research 202 (2022) 107567

Contents lists available at ScienceDirect

Electric Power Systems Research

journal homepage: www.elsevier.com/locate/epsr

Intelligent hierarchical energy and power management to control the voltage and frequency of micro-grids based on power uncertainties and communication latency

Reza Sepehrzad [a,d,e,*], Amirhossein Mahmoodi [b], Seyedeh Yosra Ghalebi [c], Ali Reza Moridi [d], Ali Reza Seifi [e]

[a] Department of Electrical Engineering, Politecnico di Milano, Milan, Italy
[b] Electrical Engineering Department, Amirkabir University of Technology, Tehran, Iran
[c] Department of Electrical Engineering, Feiz University of Higher Education, Kashan, Iran
[d] Office of Electrical Supervision, Ports and Maritime Organisation-Shahid Rajaee port complex, Bandar Abbas, Iran
[e] Department of Power and Control Engineering, Shiraz University, Shiraz, Iran

A R T I C L E I N F O

Keywords:
Intelligent energy management
Voltage and frequency control
Hybrid energy storage systems
Model predictive control
Intelligent neural networks

A B S T R A C T

This paper presents an intelligent energy management method to control the voltage and frequency at the primary and secondary control levels of micro-grids. The proposed model is based on the model predictive control (MPC) at the primary and intelligent neural network (INN) at the secondary. The purpose of this paper is to control the voltage and frequency based on the uncertainties of power generation resources and loads. In order to validate, the results of the proposed model are compared in different scenarios with other methods such as Fuzzy and PID controllers. The performance of the proposed method in primary and secondary as well as the coordination of this method with a high degree of sensitivity along with HESS and diesel generator units, in addition to increasing stability and reliability, protects the operation of the micro-grid against fluctuations based on uncertainties. The results show that this method, in addition to accuracy, has a higher operating speed than other controllers. As a result, the voltage and frequency restoration in the primary and the compensation of deviations from the reference in the secondary are associated with acceptable results. In order to validate the simulation results and experimental results are also presented.

Nomenclature

HESS	Hybrid Energy Storage System
PSO	particle swarm optimization
INN	Intelligent Neural Networks
CL	Critical Load
FL	Flexible Loads
DG	Distributed Generation
SOC	State of Charge
SDT	Strong Duality Theory
LF	Lyapunov Function
ΔP_{grid}	Grid power deviation (MW)
ΔP_{HESS}	HESS output power deviation (MW)
ΔP_{Diesel}	Diesel output power deviation (MW)
ΔP_{Load}	Load power deviation (MW)
A	System matrix
G	Control matrix
$\Psi(t)$	Matched uncertainties
$\Gamma(t)$	Mismatched uncertainties
P_{HESS}	HESS power (MW)
P_{grid}	Main grid Active Power (MW)
Q_{grid}	Main grid Reactive Power (MVAR)
S_{grid}	Main grid Apparent power (MVA)
ΔP	Active power changes (MW)
ΔQ	Reactive power changes (MVAR)
$V_{critical}$	Critical Voltage (V)
$\widehat{P}$	Predicted Active power (MW)
$\widehat{Q}$	Predicted Reactive power(MVAR)

* Corresponding author.
E-mail addresses: sepehrzad.reza@gmail.com, reza.sepehrzad@studio.unibo.it (R. Sepehrzad), amir30@aut.ac.ir.com (A. Mahmoodi), yosraghalebi@yahoo.com (S.Y. Ghalebi), moridi3@yahoo.com (A.R. Moridi), seifi@shirazu.ac.ir (A.R. Seifi).

https://doi.org/10.1016/j.epsr.2021.107567
Received 24 February 2021; Received in revised form 21 August 2021; Accepted 31 August 2021
Available online 16 September 2021
0378-7796/

P_{FL}	Flexible Loads active power (MW)
Q_{FL}	Flexible Loads reactive power (MVAR)
η_{loss}	Loss coefficients
C_{HESS}	Charging quantity (Ah/w)
$Cos\ \varphi$	Power factor
R	Speed regulation coefficient
Q_t^i	Reactive power injected into bus i (MVAR)
P_t^i	Active power injected into bus i (MW)
n	Total number of the bus
$\lvert V_t^i\rvert, \lvert V_t^j\rvert$	Voltage amplitude at bus i,j (V)
δ_t^i, δ_t^j	Corresponding voltage angle
G_{ij}	Conductance matrix
B_{ij}	Susceptance matrix
$\lvert\omega_t^i\rvert$	Absolute value of frequency at bus i (rad)
n_{Qi}, m_{Pi}	Droop gain
v^*_{odi}	Voltage generated by droop control (V)
ω_i	Angular frequency generated by droop control (rad)
v_{ni}	Nominal value of DG output voltage (V)
ω_{ni}	Nominal value of DG angular frequency (rad)
P_i	Filtered output active power (MW)
Q_i	Filtered output reactive power (MVAR)
v_{odi}, v_{oqi}	Direct and quadrature component of DG output voltage (V)
i_{ldi}, i_{lqi}	Direct and quadrature component of DG inductor current (A)
v_{idi}, v_{iqi}	Direct and quadrature component of inverter output voltage (V)
i_{odi}, i_{oqi}	Direct and quadrature component of DG output current (A)
v_{bdi}, v_{bqi}	Direct and quadrature component of DG bus Voltage (V)
r_{fi}, L_{fi}, C_{fi}	Resistance, inductance and capacitance of LC filter
r_{ci}, L_{ci}	Resistance and inductance of the coupling line
β	Charging and discharging coefficient
$\gamma_g(t)$	Parameter uncertainty
U_g, U_{HESS}	Control signals of Diesel generator and HESS
ΔV	Voltage deviation (V)
Δf	Frequency deviation (Hz)
$T_g, T_{grid}, T_{Diesel}, T_{HESS}$	Time constant (s)
K_P	Gain coefficient of power system
$\frac{\partial v_{critical_i}}{\partial P^T}$	Voltage sensitivity coefficient based on active power
$\frac{\partial v_{critical_i}}{\partial Q^T}$	Voltage sensitivity coefficient based on reactive power

1. Introduction

In recent years, the problems caused by fossil fuels in the production of electrical energy have created several environmental challenges. Therefore, researchers have proposed the idea of electrical micro-grids based on renewable energy. Micro-grids not only have the ability to cope with environmental challenges but also change the technical and economic structures of current networks [1, 2].

Although micro-grids have many advantages, the use of this idea in current distribution networks has faced operating conditions with various challenges such as: control challenges, security, reliability, flexibility, energy management and stability. Advances in the power electronics industry, as well as energy storages, have enabled micro-grids to provide attractive and reliable responses to these challenges. Therefore, it can be stated that power electronics and energy storage devices as two wings, play an essential role in the development of the micro-grid idea [3, 4, 5, 6, 7].

Control infrastructure is considered as one of the most important parts of micro-grids. Control factors in micro-grids are divided into three basic levels, which are: primary, secondary and tertiary. According to the various factors and objectives of operation as well as scheduling frameworks, each control level is responsible for meeting the set goals of the same level. Each level of control operates within its own time frame. Short-term objectives at the primary level, medium-term objectives at the secondary level and long-term objectives at the tertiary level are considered [8, 9, 10].

In recent years, with advances in the artificial intelligence industry and intelligent algorithms, micro-grids have seen significant advances in controlling key factors such as voltage, frequency, and power. Today, artificial intelligence structures and intelligent algorithms based on machine learning theories such as neural networks not only provide the optimal technical and economic utilization for micro-grid operators, but also the use of these structures will increase the degree of accuracy and reliability [11,12].

1.1. Literature review

In order to ensure the performance of micro-grid, control methods and stability analysis are crucial. In micro-grid, by increasing the levels of connection to the main grid, increasing the presence of distributed generation resources, using energy storage devices, increasing use of power electronics, using communication infrastructure and considering electricity market factors increase the complexity of their operation. Therefore, the complexities of micro-grids must be met by providing secure and reliable solutions. In [12], in addition to examining the methods of artificial intelligence, it has also stated the features and limitations of this method. This article is a comprehensive overview of the applications of this method in security assessment, stability assessment and fault detection in micro-grids. On the other hand, the challenges facing this idea such as the high requirements on data, unbalanced learning, interpretable artificial intelligence, problems in learning transfer and the strength of artificial intelligence based on the quality of communication have been examined.

In [13], a control method based on the predictive method for voltage and frequency regulation in an island micro-grid is presented. The proposed method is considered with respect to the voltage and frequency fluctuations at the moment of islanding. In this paper, by connecting different micro-grids to each other, it is possible to control the voltage and frequency fluctuations with proper distribution of active and reactive powers. In this paper, in addition to comparing the proposed method with PI controllers, the proposed method is analyzed in three scenarios in order to validate it. The results show the optimal control of voltage, frequency and control errors reduction. One of the weaknesses of this work is that although it considers the battery storage as part of the control structure, its dynamic behavior has not been studied. Basically, because the voltage and frequency must be controlled over short periods of the time, the dynamic behavior of the battery is not able to control the voltage and frequency fluctuations in instantaneous disturbances.

Ref [14] presents technical and economic analysis of energy management based on intelligent methods and machine learning theory. The goals set in this reference are based on two main objectives, which include maximizing the profit from energy exchange and also minimizing fluctuations due to the exchange Power flow between the micro-grid and the main network. Therefore, the objective function is planned based on technical and economic factors. The intelligent methods described in this reference include Genetic algorithms, Dynamic programming, ANFIS, Fuzzy systems, Support vector machine, Neural networks. In addition to comparing methods, their characteristics and limitations are also examined.

In [15], the authors have proposed an adaptive neuro-fuzzy inference system (ANFIS) model based on general micro-grid droop characteristics to control the voltage and frequency. The proposed model, independent of the effect of line impedance, has been investigated in various scenarios. Voltage and frequency are two basic parameters in electrical networks that are mainly dependent on active and reactive power fluctuations. In micro-grids based on distributed generations, the use of voltage source converters with a specific droop characteristic is common. With changes and fluctuations in load, fluctuations occur between production and consumption. These changes cause deviations in the output voltage and frequency of the converters. If these changes are large, the stability of the micro-grid may be compromised. Based on the results obtained from this study, it is possible to observe the proper performance of the proposed model against various load fluctuations. The proposed intelligent model is based on a combined neural network and fuzzy algorithm. One of the strengths of the proposed model is the intelligence and micro-grid learning ability against fluctuations affecting voltage and frequency changes, which in turn increases the layers studied in the neural network structure. Although this structure has good results in island micro-grids, but the validation of this structure has not been analyzed in the grid connected operation mode as well as networked micro-grids. On the other hand, the absence of storage resources, which play an essential role in controlling the power fluctuations, is a significant part that challenges the proposed structure.

In [16], a new method for controlling voltage and frequency in AC micro-grid in the presence of wind farms based on synchronous generators is presented. The proposed technique allows the wind farm to be connected to the main grid using an HVDC rectifier. The control model presented in this paper allows the AC micro-grid, which consists of a wind farm and a rectifier, to be operated in two modes of voltage or current control. Among the strengths presented in the proposed model are endurance against load fluctuations in the island operation mode, resistant to capacitive bank switching, resistant to power generation constraints due to low wind speed and also AC rectifier switching. One of the major challenges facing this model is its efficiency in hybrid micro-grid structures based on DC power generation resources. This is important because the hybrid micro-grid structure in addition to many advantages, has a variety of control complexities.

In [17], the authors have presented a control model based on compensation of the voltage and frequency deviations in the secondary level of island micro-grids by considering the active power distribution. The proposed model based on multi-objective functions considers the effects of model uncertainty and changing the parameters of power generation units. It thus offers a certain degree of strength against all these factors. In the proposed model, in order to control voltage and frequency fluctuations, the information of distributed generation units and the resources that are in their neighborhood are considered. This method not only simplifies communications infrastructure, but also reduces investment and operating costs. The proposed design counteracts any fluctuations in the terminal voltage and frequency of DG units. This method also facilitates various errors based on the optimal division of active power in a predetermined ratio, despite the variations of variable load over time. The proposed control scheme is based on a nonlinear dynamic model of inverter-based DG units (which may not all be the same). One of the ambiguities in this research is the lack of validation of the proposed model in the grid connected mode. On the other hand, in the inverter-based micro-grids, the imbalance between production and consumption causes a deviation in the voltage and output frequency of these converters, which in the absence of a proper micro-grid control strategy will be unstable.

In [18], the authors have proposed a model for voltage and frequency control of an islanded micro-grid at the secondary level based on the finite time factor. The proposed model compensates for the voltage and frequency deviations from their reference values by controlling the active and reactive power flow. Therefore, it has presented its goals by properly distributing active and reactive power as well as using communication infrastructure based on local information and neighborhoods. Therefore, the communication structure used in this research is designed based on the neighbor-to-neighbor protocol. The strengths of this research based on the results are: the efficiency of the proposed model by considering the unequal impedances of the lines and also control of the load fluctuations and operation in the plug and-play mode.

In [19], a new multilayer architecture is designed for the control algorithm based on the large signal model, which enables the micro-grid to operate in a wide range of operating points. The objectives of the designed controllers include voltage and frequency amplitude regulation as well as the output power of distributed generation sources. In this paper, two levels of local and centralized control are considered. The operation scenario of these controllers is based on communication structures. The performance of the proposed method is such that when the central controllers are unable to operate due to errors in the communication networks, then the local controllers must control the critical micro-grid factors. The voltage and frequency control method is based on the modified droop method and is considered in the distribution network with high R/X rate. The inner layer of the proposed model is responsible for regulating voltage and frequency, while the outer layer is responsible for controlling the distribution and exchange of power. This model has also been analyzed for validation in three scenarios of islanded, grid connected and networked mode. One of the strengths of this paper is the reduction of uncertainties in the energy distribution management system by exchanging power in the networked mode micro-grid operation structure. One of the ambiguities in this article is the lack of accurate study of the impact of errors in the communications infrastructure and how the proposed model works with such errors. On the other hand, not examining the effect of communication infrastructure delays and the resulting uncertainties on the proposed method also poses a major challenge to this model.

In [20], a new demand response (DR) control method is proposed to control frequency fluctuations by considering the compensation of problems caused by communication delay and frequency deviation error detection. In this paper, a centralized and distributed control method based on flexible loads is programmed. The results of the proposed method show the reduction of the maximum frequency deviation.

1.2. Micro-grid research challenges

As mentioned in the literature review section of previous research [1-20], the weaknesses of research have been categorized. Some of the most important research challenges related to micro-grids can be expressed as follows:

1) As the number of micro-grids connected to the main grid increases, controlling and monitoring the power flow between the micro-grids and the main grid will become more complex. Therefore, lack of management and control of exchange power will lead to stability problems and reduced reliability in the operation of energy distribution networks in the presence of multiple micro-grids.
2) Since the voltage and frequency are considered as one of the most important factors of operation and stability, control of these two factors in the period of milliseconds and seconds is essential. Due to the fact that the micro-grid has the feature of operation in two modes of connection to the main grid and islanded, so it is very important to provide an efficient model in controlling the voltage and frequency, especially in switching time intervals between these two modes of operation. At the same time, it should be noted that the operation method in these two cases is so different from each other that this should also be considered in providing a control method. For example, when the micro-grid is operated as a connection to the main network, the frequency deviation range of about 1% (0.5 Hz) is considered. While this deviation in islanded mode is equal to 3% (1.5 Hz) [8,11].
3) Because synchronizing the voltage amplitude between the micro-grid and the main grid is complex, connecting two active electrical grids with different voltage amplitudes create a surge current between two grids. This in turn will lead to stability problems and reduced reliability.
4) The connection of the micro-grid to the main grid will cause the dependence of the micro-grid power, while in the case of islands, the micro-grid power will be independent. Algorithm for changing power independence as well as power dependence between these two systems is another issue that should be considered in

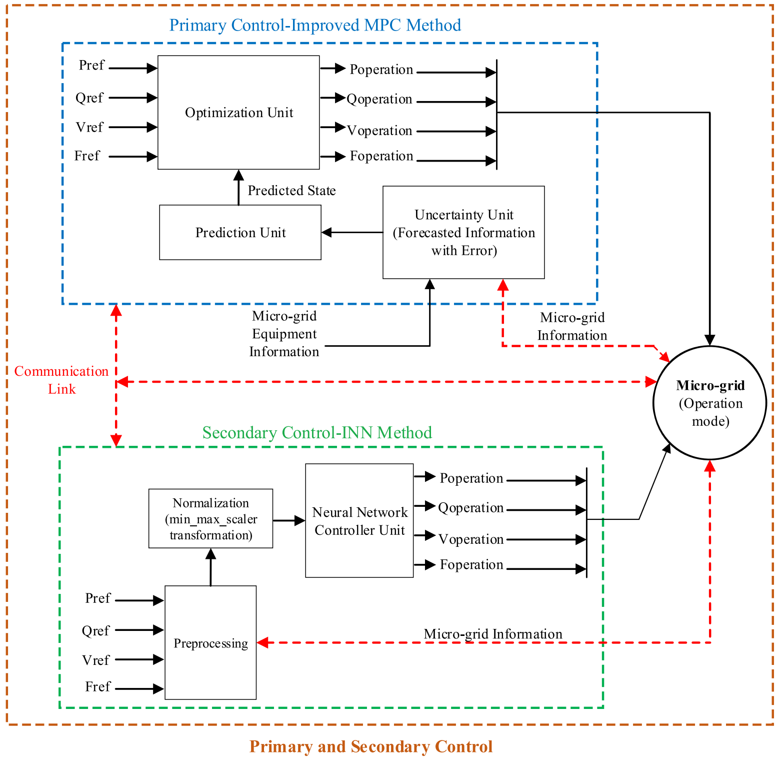

Fig. 1. The structure of the proposed control model in the presence of communications infrastructure

providing methods of energy management and micro-grid power control.

5) Because the micro-grid includes various devices such as distributed generation sources, energy storage devices, power electronics, communication infrastructure and electrical loads with different characteristics, providing a control structure appropriate to the characteristics of the equipment in the micro-grid is difficult and vital. In other words, it can be said that due to the complexities of micro-grids, the presentation of control models in addition to high importance, has both potential and actual complexity.
6) Distribution and management of power between power generation sources, energy storage and consumers due to their inequality coefficient of coincidence, controlling the voltage and frequency of the micro-grid becomes complex and difficult in different operating conditions.
7) Problems due to the lack of fast and accurate error detection in the micro-grid, which exploits it in network connection modes and islanded mode leads to unstable conditions.
8) With the increase of micro-grid penetration in current networks in order to monitor and control optimally at different levels of micro-grids, conventional methods do not have sufficient capability. Therefore, the use of intelligent and advanced methods is essential.
9) Lack of fast and accurate investigation, prediction and monitoring of dynamic micro-grid behavior based on transient events, provide critical operation problems. Transient factors can be divided into the following two categories, which it is necessary to consider these factors in presenting control models: **Normal transient factors**: load step, motor starting, switching, load shedding, transformer inrush, etc. **Unexpected disturbances**: sudden power outage, short circuit, etc.
10) Lack of investigation and consideration the uncertainties affecting the dynamic behavior of the micro-grid, which poses critical problems for the stability and management of the micro-grid.

1.3. Research objectives and innovation

Part 1: In this paper, an attempt has been made to consider various factors that affect the performance and operation of the micro-grid. The proposed method is based on the management and control of power and energy with the aim of controlling the voltage and frequency of the micro-grid. Then, by using predictive and intelligent models, increasing the level of accuracy and speed of the proposed method in detecting different events and providing an appropriate reaction based on uncertainties is presented. Meanwhile, with the optimal management of power distribution based on intelligent frameworks, on the one hand, power exchange with the main network and on the other hand, power management between energy production sources, storages and consumers is controlled. In this regard, by considering the predictive dynamic model of some equipment, the speed and accuracy of the proposed method in dealing with various events has increased.

Part 2: In this paper, the proposed model is based on controlling the operation objectives in primary and secondary micro-grids, using predictive model and intelligent algorithm. The two main factors in the primary and secondary levels are the voltage and frequency fluctuations control. These two factors are considered as two important parameters in the operation of the micro-grid. At the primary level, the control method must control the instantaneous fluctuations of voltage and frequency. At the secondary level, the deviation of these two parameters from their reference values is controlled by the proposed method. At the primary level, voltage and frequency parameters are controlled using a prediction model based on uncertainties as well as the use of optimization tools along with the optimal performance of energy storage units. At the secondary level, voltage and frequency deviation relative to reference values are controlled using an intelligent control method based on neural network algorithm and analysis of micro-grid data. The effective factors in the proposed model are the analysis of the dynamic behavior of the hybrid energy storage system (HESS) and the backup diesel generator in the active and reactive power distribution. In addition, the proposed model is based on the use of communications infrastructure. The simulation and experimental results of the proposed method along with control algorithms have been analyzed to evaluate the efficiency of this method. Fig. 1 shows the proposed control structure in this paper.

The **main innovations** of this article are summarized below:

1 Presenting a robust voltage and frequency control model based on predictive control structure at the primary level and INN algorithm at the secondary level by considering the uncertainty of distributed generation sources, loads, communication delays and the role of flexible loads in managing critical scenarios.
2 Presenting the optimal active and reactive power distribution model and intelligent energy management between power generation sources and HESS in order to respond appropriately to the control of voltage and frequency fluctuations in both primary and secondary levels by considering the charge, discharge and SOC thresholds of HESS.
3 Increasing the speed and accuracy of the criteria to compensate for instantaneous voltage and frequency fluctuations, as well as reducing the standard deviation from the reference values of voltage and frequency by intelligent and predicted structure.
4 Increasing detection speed as well as high accuracy in dealing with events affecting the operation of the micro-grid

The rest of the article includes sections: In section 2, modeling of micro-grid parameters along with the control method in primary and secondary is stated. Section 3 describes the simulation and implementation requirements. Section 4 describes the results. Finally, a conclusion is presented in Section 5.

2. Modeling and control topology

2.1. Network model and equipment

2.1.1. Main grid model

Eqs. (1)-(2) show the power flow model between the micro-grid and the main network as well as the critical voltage prediction model of the micro-grid during operation based on the linear model by Taylor approximation [21-22]. In Eq. 2, the sensitivity coefficients $\frac{\partial v_{critical_i}}{\partial P^T}$, $\frac{\partial v_{critical_i}}{\partial Q^T}$ are calculated according to the Ref [22].

$$\begin{bmatrix} P_{grid-\min} \le P(t) \le P_{grid-\max} \\ Q_{grid-\min} \le Q(t) \le Q_{grid-\max} \end{bmatrix}, \forall t \Rightarrow (P_{grid}(t))^2 + (Q_{grid}(t))^2 \le (S_{grid-\max})^2 \tag{1}$$

$$\widehat{V}_{critical_i}[k] = \begin{bmatrix} V_{critical_i}[0] + \frac{\partial v_{critical_i}}{\partial p^T_{DG}} \cdot \Delta P_{DG}[k] + \frac{\partial v_{critical_i}}{\partial Q^T_{DG}} \cdot \Delta Q_{DG}[k] + \frac{\partial v_{critical_i}}{\partial p^T_{HESS}} \cdot \Delta P_{HESS}[k] \\ + \frac{\partial v_{critical_i}}{\partial p^T_{grid}} \cdot \Delta P_{grid}[k] + \frac{\partial v_{critical_i}}{\partial Q^T_{grid}} \cdot \Delta Q_{grid}[k], \forall i, k \end{bmatrix} \tag{2}$$

2.1.2. Model of distributed generation resources

Since renewable energy resources such as solar and wind have uncertainty due to oscillating behavior in power generation, so using the uncertainty model, their probability density function can be modeled. In order to simplify the calculations of the probability function, this problem can be considered as convex and limited predictive distances. This model is obtained according to data based on information of power generation sources and their operation [23-24]. Since in micro-grids, reactive and active powers are used as controllable parameters in voltage and frequency regulation, so regardless of their dynamic model, these two factors are modeled in Eqs. (3) to (5). The time model considered in this research is in seconds. As a result, reactive power can be considered equivalent to$Q_{DG}[k] = Q_{DG-ref}[k]$. The predictive power distribution equations based on the predicted ranges are as follows:

$$\begin{bmatrix} P_{DG-\min} \le P[k] \le P_{DG-\max} \\ Q_{DG-\min} \le Q[k] \le Q_{DG-\max} \end{bmatrix}, \forall t \Rightarrow \begin{bmatrix} (P_{DG}[k])^2 + (Q_{DG}[k])^2 \le (S_{DG}[k])^2 \\ (P_{DG}[k])^2 + (Q_{DG}[k])^2 \le (3V_{DG}[k] I_{rms-DG})^2 \end{bmatrix} \tag{3}$$

$$\begin{aligned} &\widehat{P}_{DG}[k] + \Delta P_{DG-\min}[k] \le \widehat{P}_{DG}[k] \le \widehat{P}_{DG}[k] + \Delta P_{DG-\max}[k], \forall k \\ &Q_{DG-\min}[k] \le \widehat{Q}_{DG}[k] + \Delta Q_{DG}[k] \le Q_{DG-\max}[k], \forall k \end{aligned} \tag{4}$$

$$\begin{aligned} \Delta P_{DG}[k] &= P_{DG}[k] - P_{DG}[0] \\ \Delta Q_{DG}[k] &= Q_{DG}[k] - Q_{DG}[0] \end{aligned} \tag{5}$$

2.1.3. Flexible load model

One of the important factors in controlling the voltage and frequency of the micro-grid is flexible loads. Therefore, part of the micro-grid load is considered as flexible loads. Flexible loads play their role in critical situations based on management logics [25]. Although the use of flexible load model improves the economic factors of the network, in order to operate efficiently, proper control over this part of the micro-grid must be provided [26].The model for these loads is based on the rules of time shift and load shedding. In this study, in addition to the set of flexible loads, critical loads are also considered. The planned power for critical loads is 0.44MW. In order to increase the micro-grid security level, the power of the HESS unit is considered equal to the critical loads. The flexible load model is as follows:

$$P_{FL-\min} \le P_{FL-(t)} \le P_{FL-\max}, \forall t \tag{6}$$

$$\sqrt{(Q_{FL-(t)})^2 + (P_{FL-(t)})^2} * |\cos\phi| = |P_{FL-(t)}|, \forall t \tag{7}$$

2.1.4. Power flow model

The main and micro-grid AC power flow model based on power, voltage and frequency constraints are equal to [27]:

$$P^i_t = \sum_{j=1}^{n} |V^i_t||V^j_t| (G_{ij}\cos(\delta^i_t - \delta^j_t) + B_{ij}\sin(\delta^i_t - \delta^j_t) \tag{8}$$

$$Q^i_t = \sum_{j=1}^{n} |V^i_t||V^j_t| (G_{ij}\sin(\delta^i_t - \delta^j_t) + B_{ij}\cos(\delta^i_t - \delta^j_t) \tag{9}$$

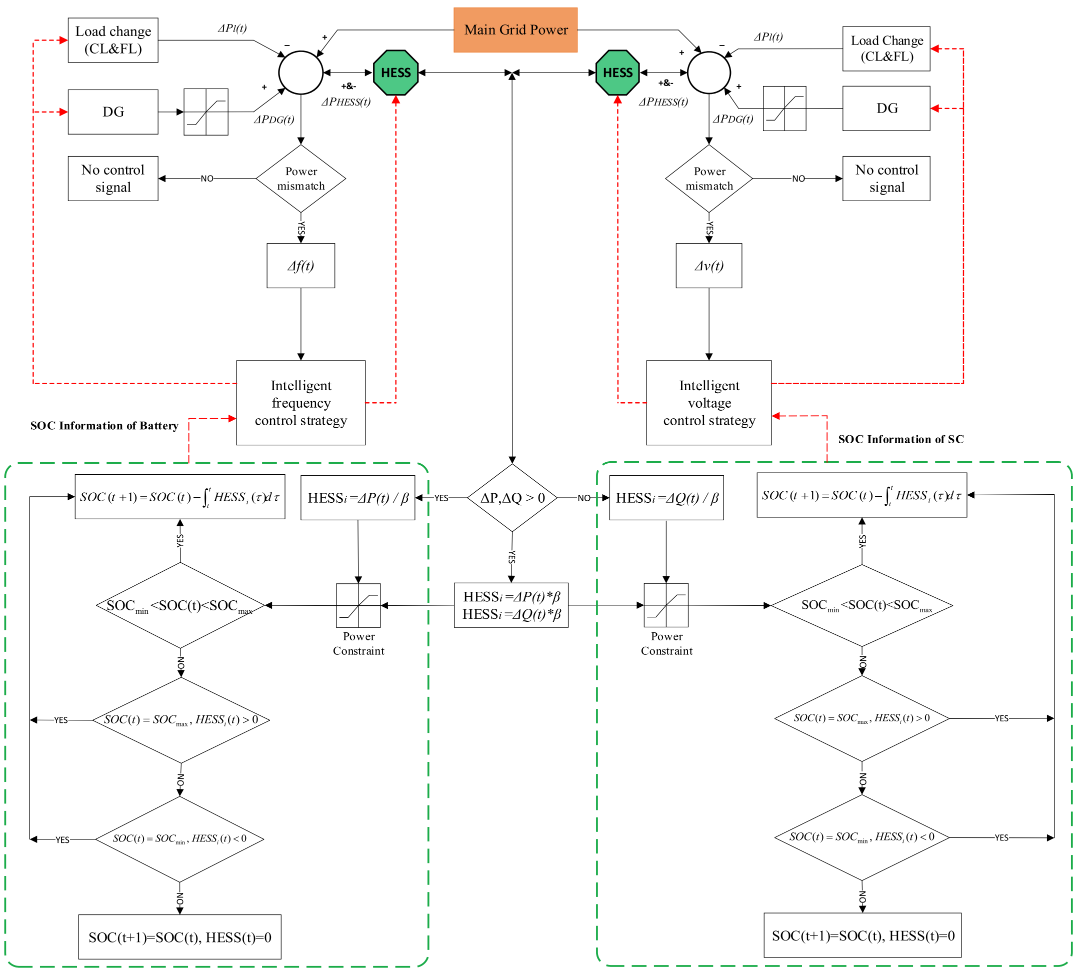

Fig. 2. SOC flowchart - primary and secondary level control units

$$\left\{\begin{array}{l} P_t^{ij} = \left|V_t^i\right|\left\{\left|V_t^i\right|G_{ij} - \left|V_t^j\right|\left(G_{ij}\cos\left(\delta_t^i - \delta_t^j\right) + B_{ij}\sin\left(\delta_t^i - \delta_t^j\right)\right)\right\} \\ Q_t^{ij} = -\left|V_t^i\right|\left\{\left|V_t^i\right|B_{ij} + \left|V_t^j\right|\left(G_{ij}\cos\left(\delta_t^i - \delta_t^j\right) - B_{ij}\sin\left(\delta_t^i - \delta_t^j\right)\right)\right\} \end{array}\right\} \Rightarrow \left(P_t^{ij}\right)^2 + \left(Q_t^{ij}\right)^2 \leq \left(S_{\max}^{ij}\right)^2 \tag{10}$$

$$\left|V^i\right|_{\min} \leq \left|V_t^i\right| \leq \left|V^i\right|_{\max} \tag{11}$$

$$\left|\omega^i\right|_{\min} \leq \left|\omega_t^i\right| \leq \left|\omega^i\right|_{\max} \tag{12}$$

2.1.5. Dynamic model of power control and electronic converters of DG units

The model of DG unit converter controllers is based on Droop characteristics, especially at the time of islanding. The equations of the electronic converter model are expressed according to [28]. The factors expressed in this section are the infrastructure of the proposed control model at the secondary level.

$$v_{odi}^{*} = v_{ni} - n_{Qi}Q_i \tag{13}$$

$$\omega_i = \omega_{ni} - m_{Pi}P_i \tag{14}$$

$$\frac{d}{dt}\left(i_{ldi}\right) = -\frac{r_{fi}i_{ldi}}{L_{fi}} + \omega_i i_{lqi} + \frac{v_{idi}}{L_{fi}} - \frac{v_{odi}}{L_{fi}} \tag{15}$$

$$\frac{d}{dt}\left(i_{lqi}\right) = -\frac{r_{fi}i_{lqi}}{L_{fi}} - \omega_i i_{ldi} + \frac{v_{iqi}}{L_{fi}} - \frac{v_{oqi}}{L_{fi}} \tag{16}$$

$$\frac{d}{dt}\left(v_{odi}\right) = \omega_i v_{oqi} + \frac{i_{ldi}}{C_{fi}} - \frac{i_{odi}}{C_{fi}} \tag{17}$$

$$\frac{d}{dt}\left(v_{oqi}\right) = -\omega_i v_{odi} + \frac{i_{lqi}}{C_{fi}} - \frac{i_{oqi}}{C_{fi}} \tag{18}$$

$$\frac{d}{dt}\left(i_{odi}\right) = -\frac{r_{ci}i_{odi}}{L_{ci}} + \omega_i i_{oqi} + \frac{v_{odi}}{L_{ci}} - \frac{v_{bdi}}{L_{ci}} \tag{19}$$

$$\frac{d}{dt}\left(i_{oqi}\right) = -\frac{r_{ci}i_{oqi}}{L_{ci}} - \omega_i i_{odi} + \frac{v_{oqi}}{L_{ci}} - \frac{v_{bqi}}{L_{ci}} \tag{20}$$

2.1.6. HESS and diesel generator dynamic model

Another important factors that play a key role in controlling the voltage and frequency of the micro-grid are the HESS units and their dynamic model to compensate the voltage and frequency fluctuations. It is noteworthy that the power of the HESS unit and the diesel generator has been selected in such a way that part of this power is considered as a spinning reserve in order to control the voltage and frequency. In this section, the transfer function model: diesel generator, governor, HESS unit and main power system are expressed in Eqs. (21) to (24).

$$G_{Diesel} = 1 \,/\, \left(T_{Diesel}s + 1\right) \tag{21}$$

$$G_g = 1 \,/\, \left(\left(T_g + \sigma_g(t)\right)s + 1\right) \tag{22}$$

$$G_{HESS} = 1 \,/\, \left(T_{HESS}s + 1\right) \tag{23}$$

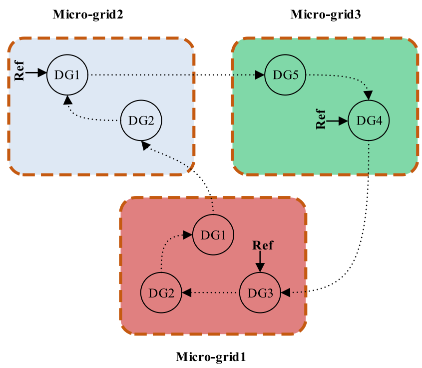

Fig. 3. Unidirectional graph communication model in different zones

Table 1
Characteristics of communication infrastructure

A set of communication nodes that is equivalent to the DGs in the micro-grid.	**Infinite and non-empty set**	$V = \{v_1, v_2, \cdots, v_N\}$
Send information from node i to node j	Set of edges	$E = \{(E_j, E_i)\}$
The weight of edge conditions are as follows: $a_{ij} > 0$ *if* $(v_i, v_j) \in E$ *otherwise* $a_{ij} = 0$	Associated adjacency matrix	$A = [a_{ij}] \in \mathrm{R}^{N\times N}$

$$G_{grid} = k_{grid} \big/ \left(T_{grid}s + 1\right) \tag{24}$$

The frequency dynamic model based on uncertainty due to the change of governor parameters during the operation of the diesel generator is considered with respect to $\sigma_g(t)$ and the time constant T_g. The dynamic equations of frequency with respect to the parameters affecting it are as follows:

$$x(t) = \left[\Delta f(t), \Delta P_{Diesel}(t), \Delta P_{HESS}(t), \Delta P_g(t)\right]^T \in \mathrm{R}^m \tag{25}$$

$$\frac{d}{dt}(\Delta f(t)) = \frac{k_{grid}}{T_{grid}}\left[\Delta P_{Disel}(t) + \Delta P_{HESS}(t) + \Delta P_{grid}(t) - \Delta P_{Load}(t)\right] - \frac{1}{T_{grid}}\Delta f(t) \tag{26}$$

$$\frac{d}{dt}(\Delta P_{Diesel}(t)) = -\frac{1}{T_{Diesel}}\Delta P_{Diesel}(t) + \frac{1}{T_{Diesel}}\Delta P_g(t), \tag{27}$$

$$\frac{d}{dt}\left(\Delta P_g(t)\right) = \frac{\sigma_g(t)}{T_g\left(T_g + \sigma_g(t)\right)}\left[\frac{1}{R}\Delta f(t) + \Delta P_g(t) - u_g(t)\right] - \frac{1}{RT_g}\Delta f(t) - \frac{1}{T_g}\Delta P_g(t) + \frac{1}{T_g}u_g(t) \tag{28}$$

$$\Delta P_{HESS}(t) = \frac{1}{T_{HESS}}u_{HESS}(t) - \frac{1}{RT_{HESS}}\Delta f(t) - \frac{1}{T_{HESS}}\Delta P_{HESS}(t) \tag{29}$$

As shown in Eq. (28), the uncertainty factor based on changes in diesel generator parameters during operation is equivalent to:

$$\gamma_g(t) = \sigma_g(t) \big/ \left[T_g + \left(T_g + \sigma_g(t)\right)\right] \tag{30}$$

According to Eqs. (25) to (30), another classification can be described for the uncertainties based on the diesel generator ($\gamma_g(t)$) and the power system ($\Delta P_{Load}(t)$and$\Delta P_{grid}(t)$). These categories include matched ($\Psi(t)$) and mismatched ($\Gamma(t)$) uncertainties. Therefore, the frequency dynamic model is equal to:

$$x^{'}(t) = Ax(t) + G(u(t) + \Psi(t) + \Gamma(t)) \tag{31}$$

$$A = \begin{bmatrix} \frac{1}{T_{grid}} & \frac{k_{grid}}{T_{grid}} & 0 & \frac{k_{grid}}{T_{grid}} \\ 0 & -\frac{1}{T_{Diesel}} & \frac{1}{T_{Diesel}} & 0 \\ -\frac{1}{RT_g} & 0 & -\frac{1}{T_g} & 0 \\ -\frac{1}{RT_{HESS}} & 0 & 0 & -\frac{1}{T_{HESS}} \end{bmatrix}, G = \begin{bmatrix} 0 & 0 \\ 0 & 0 \\ \frac{1}{T_g} & 0 \\ 0 & \frac{1}{T_{HESS}} \end{bmatrix}, \Psi(t) = \begin{bmatrix} -T_g\lambda_g(t)u_g(t) \\ 0 \end{bmatrix}, \Gamma(t) = \begin{bmatrix} 0 & \frac{k_{grid}}{T_{grid}}\left(\Delta P_{grid} - \Delta P_{Load}(t)\right) \\ & 0 \\ & \lambda_g(t)\left(\frac{1}{R}\Delta f + \Delta P_g(t)\right) \\ & 0 \end{bmatrix} \tag{32}$$

$$u(t) = \left[u_g(t), u_{HESS}(t)\right]^T \in \mathrm{R}^n \tag{33}$$

2.1.6.1. SOC Model of HESS. In order to investigate the SOC behavior of HESS in this paper, two models are analyzed according to Fig. 2. The first model is related to the voltage and frequency restoration. The second model is related to the power flow of distributed generation resources. If SOC (0) is considered as initial values and HESS energy changes are considered in the time interval t, then the SOC equations in other time ranges are equal to:

$$SOC(t+1) = \begin{cases} SOC(t) - \int_0^t HESS(\tau)d\tau, & SOC_{\min} < SOC(t) < SOC_{\max}, or \\ & SOC(t) = SOC_{\max} \& HESS_i(t) > 0, or \\ & SOC(t) = SOC_{\min} \& HESS_i(t) < 0, \\ SOC(t), & else, \end{cases} \tag{34}$$

$$HESS(t) = \begin{cases} \Delta P_{HESS-\max}/\beta, & \Delta P_{HESS}(t) > \Delta P_{HESS-\max}, \\ \Delta P_{HESS}(t)/\beta, & 0 < \Delta P_{HESS}(t) \le \Delta P_{HESS-\max}, \\ \beta\Delta P_{HESS}(t), & \Delta P_{HESS-\min} \le \Delta P_{HESS}(t) < 0, \\ \beta\Delta P_{HESS-\min}, & \Delta P_{HESS}(t) < \Delta P_{HESS-\min}, \end{cases} \quad HESS(t) = \begin{cases} \Delta Q_{HESS-\max}/\beta, & \Delta Q_{HESS}(t) > \Delta Q_{HESS-\max}, \\ \Delta Q_{HESS}(t)/\beta, & 0 < \Delta Q_{HESS}(t) \le \Delta Q_{HESS-\max}, \\ \beta\Delta Q_{HESS}(t), & \Delta Q_{HESS-\min} \le \Delta Q_{HESS}(t) < 0, \\ \beta\Delta Q_{HESS-\min}, & \Delta Q_{HESS}(t) < \Delta Q_{HESS-\min}, \end{cases} \tag{35}$$

2.1.6.2. Predictive model of charge and discharge of HESS with operating constraints. As mentioned, one of the roles of the HESS is to restore the voltage and frequency of the micro-grid. Therefore, the prediction model of the HESS charge and discharge along with operating constraints is expressed in Eqs. (36) to (39):

$$SOC[k] = C_{HESS}[k]/C_{HESS-\max} \Rightarrow [C_{ESS}[k-1] - (\eta_{loss} * C_{HESS}[k-1]) - (P_{HESS}[k-1]) * \Delta t]/C_{HESS-\max} \tag{36}$$

$$\Delta P_{HESS}[k] = P_{HESS}[k] - P_{HESS}[0] \tag{37}$$

$$C_{HESS-\min} \le C_{HESS}[k] \le C_{HESS-\max} \Rightarrow P_{HESS-\min} \le P_{HESS}[k] \le P_{HESS-\max} \tag{38}$$

$$|\Delta P_{HESS}[k]| \le \Delta P_{HESS-\max} \tag{39}$$

2.1.7. Communication infrastructure model

Since communication infrastructure is one of the underlying factors in micro-grid management and control, so according to Fig. 3 in this paper, the unidirectional graph model along with the delay model in communication infrastructure has been used. One of the scenarios discussed in the results section is based on the effect of communication latency on the proposed control method. The communication delay

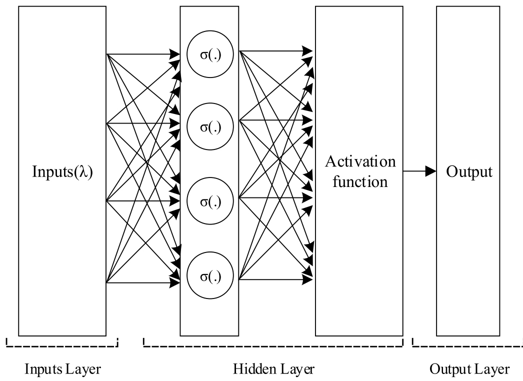

Fig. 4. Structure of INN algorithm

model is considered based on the method presented in the reference [29]. The unidirectional graph model is described in (40).

$$\begin{cases} G_{graph} = (V, E, A) \\ \overline{\omega}'_i(t) = \omega'_i(t) \sum d_{\omega ij} \left[\overline{\omega}_i(t - \tau_i(t)) - \overline{\omega}_j(t - \tau_j(t)) \right] \end{cases} \tag{40}$$

where $\tau(t)$ is the time-varying delay which is defined in the $0 < \tau(t) < \tau_{\max}(t)$range,$\tau_{\max}(t)$ is the maximum communication delay tolerance. Table 1

2.2. Voltage and frequency control modeling at primary and secondary

2.2.1. Voltage and frequency model at the primary control

2.2.1.1. The principle of MPC. In this section, the voltage and frequency control model based on predictive control theory is presented. Different sections such as objective function, problem solving method and linearization are expressed. Predictive control model based on uncertainties of power generation sources and electrical loads are considered. Considering the uncertainties in this model increases the efficiency of the proposed method. Accordingly, in this section, the model of a time-invariant discrete linear system with limited uncertainty and constraints of its time domain is expressed [30-32]:

$$\begin{cases} x(k+1) = Ax(k) + B_u u(K) + B_l \omega(k) \\ z(k+1) = C(k) + D_u u(K) + D_l \omega(k) \end{cases} \tag{41}$$

$$\begin{aligned} |u_r(k+i)| &\le u_{r,\max}, i \ge 0, r = 1, 2, ..., m \\ |x_r(k+i)| &\le x_{r,\max}, i \ge 1, r = 1, 2, ..., m \end{aligned} \tag{42}$$

Where $x(k) \in R^n$: is the system state, $u(k) \in R^m$: is the input, $z(k) \in R^p$:is the output of the system, $w(t) \in$ W: indicates uncertainty due to errors and external disturbances expressed by the mismatch model. $W \in R^n$, $X \in R^n$, $U \in R^n$are compact, convex, and contain an open neighborhood of the origin, respectively. Therefore, the objective function of the predictive model can be considered as a *min-max* function. By solving Eqs. (41) to (43), the values of control variables are obtained in the next time period.

$$\begin{aligned} &\underset{u\in U\ w\in W}{minmax} J_{Tp}(k) \Rightarrow \underset{u\in U\ w\in W}{minmax} \sum_{i=0}^{T_P} [\,\| x(k+i)\|_T + \| u(k+i)\|_R] \\ &therefore \Rightarrow U_k = \{u(k+1), u(k+2), ..., u(k+T_p-1)\} \end{aligned} \tag{43}$$

Where *U:* is the set of control variables, *W:* is the admitted disturbances set, $T_{p:}$ is the number of prediction horizons, *R* and *T*: is the diagonal weighting matrices, $U_{k:}$ is the set of the state feedback control law of the next time periods, *u(k+1)* is the first optimal reaction in the next control step.

Using the model expressed in Eqs. (41) to (43), it is possible to apply the minimization of the voltage and frequency fluctuations at the primary level of micro-grids. Input variables include active and reactive micro-grid powers. State variables are also considered as node voltages and micro-grid frequencies. The disturbance variables are also considered as active and reactive power fluctuations of power generation sources and HESS units. Therefore, by solving the proposed model, the modified powers are sent to the power generation units and the HESS units. The strength of this model in terms of power generation, is that the operator of the micro-grid at different times can consider various strategies to control voltage and frequency based on active and reactive power. Power fluctuations are generally predictable at primary. Therefore, in order to control voltage and frequency fluctuations, this model can have high efficiency.

$$\text{minmax} \begin{bmatrix} \sum_{k=1}^{N_P} \Big(\| \widehat{V}_{critical}[k] - V_{ref} \|^2_{W_V} + \| \widehat{f}[k] - f_{ref} \|^2_{W_f} + \| SOC[k] - SOC(0) \|^2_{W_{SOC}} + \\ \| \Delta Q_{DG}[k] - \Delta Q_{DG}[k-1] \|^2_{W_{Q-DG}} + \| \Delta P_{DG}[k] - \Delta P_{DG}[k-1] \|^2_{W_{P-DG}} + \| \Delta P_{HESS}[k] - \Delta P_{HESS}[k-1] \|^2_{W_{HESS}} \\ + \| \Delta P_{Load}[k] - \Delta P_{Load}[k-1] \|^2_{W_{Load}} + \| \Delta P_{grid}[k] - \Delta P_{grid}[k-1] \|^2_{W_{grid}} \Big) \end{bmatrix} \tag{44}$$

2.2.1.2. Objective function of the voltage and frequency control model based on MPC method. The goals in primary control are to restore and control the voltage and frequency fluctuations. The MPC is used to control these two factors in the next time horizons of micro-grid operation. The control model should basically be coordinated with the

Table 2
Summary of INN training structure

Item	Value
No. of hidden layers	**1-3**
No. of neurons in each layer	**1000**
Loss function	**Mean square error pluse L_2**
Learning rate	**$1e^{-2}$**
Exponential decay rate	**0.96**
Exponential decay step	**50**
No. of training samples	**87501**
No. of test samples	**1000- 2400**
Iteration steps	**2000**
Data preprocessing	**min-max-scaler**

Table 3
Time calculations comparing INN and Monte Carlo methods

No. of samples	Calculation time	
	INN	Monte Carlo
1000	0.8	12.35
2000	1.01	16.25
5000	1.21	20.82
8000	1.6	30.44

cooperation between power generation units and HESS. It should also be noted that power generation units are assumed to be operated in MPPT mode. Basically, the control variables based on the active and reactive power factors of DG units as well as the rules of charging and discharging HESS sources based on their optimal SOC are considered. In addition, in order to increase the accuracy in the calculations of the proposed model, other influential factors such as the effect of loads and the main grid power are also expressed in the objective function.

Where $\widehat{V}_{critical}[k]$: is the predicted critical voltage at the *k-th* prediction period, V_{ref}:is the micro-grid reference voltage, $\widehat{f}[k]$: is the predicted frequency at the *k-th* prediction period, f_{ref}: is the micro-grid reference frequency, $SOC[k]$: is the HESS state of charge, $SOC(0)$: is the Initial value, W: is the diagonal weight matrices for each of the parameters in the objective function.

In order to control voltage and frequency fluctuations, the voltages of micro-grid nodes are considered as global and local. The important point is to determine the critical voltage of the micro-grid bus. Ref [33] provides an efficient method for measuring and determining the critical bus. The range of voltage fluctuations as well as protection voltages is expressed according to IEEE 1159-2009 standard. Therefore, the operation of micro-grids in different zones is considered. Each zone is operated based on reference voltage and frequency. Therefore, according to Fig. 3, three categories of micro-grids are considered.

2.2.1.3. Solution method

2.2.1.3.1. Solution method for robust optimization model. In the optimization model, the most critical state of uncertainties (sudden changes in the output of power sources and loads) is considered in order to increase the reliability and security of the micro-grid. Because solving Eq. (45) is complex and difficult, it is necessary to transfer this equation into a single-level equation. Here, using strong duality theory, Eq. (45) can be transformed into a single-level- quadratic optimization equation [34].

$$\left\{\begin{array}{l} \min_{u}\max_{w} f(u,w) \\ s.t. Au+Bw\leq C \\ w\in\left[\widehat{w}+\Delta w_{lower},\widehat{w}+\Delta w_{upper}\right] \\ u\in\left[u_{lower},u_{upper}\right]\end{array}\right\}\Rightarrow\left\{\begin{array}{l} \min_{u} f(u,w) \\ s.t. Au+\max_{w} Bw\leq C \\ w\in\left[\widehat{w}+\Delta w_{lower},\widehat{w}+\Delta w_{upper}\right] \\ u\in\left[u_{lower},u_{upper}\right]\end{array}\right\} \tag{45}$$

The single-level Eq. (45) is expressed according to Eq. (47).

$$\begin{array}{l} strongdualitytheory \Rightarrow A_i u + B_i w \leq A_i u + B_i(\widehat{w} + \Delta w_{lower}) + 1^T\theta_i \\ \Rightarrow \left\{\begin{array}{l} \min_{\theta_i} A_i u + B_i(\widehat{w} + \Delta w_{lower}) + 1^T\theta_i \\ s.t. \quad \theta_i \geq B_i\left(\Delta w_{upper} - \Delta w_{lower}\right) \\ \qquad \theta_i \geq 0 \end{array}\right\}, \left\{\begin{array}{c} A_i u + \max_{\mu}(B_i\left(\widehat{w} + \Delta w_{lower} + \mu\left(\Delta w_{upper} - \Delta w_{lower}\right)\right) \leq C_i \\ 0 \leq \mu \leq 1 \end{array}\right\} \end{array} \tag{46}$$

$$\left\{\begin{array}{ll} & \min_{u} f(u,w) \\ s.t. & A_i u + B_i(\widehat{w} + \Delta w_{lower}) + 1^T\theta_i \leq C_i \\ & \theta_i \geq B_i\left(\Delta w_{upper} - \Delta w_{lower}\right) \\ & \theta_i \geq 0 \\ & u_{lower} \leq u \leq u_{upper} \end{array}\right\} \tag{47}$$

$$\begin{array}{l} f\left(\Delta P_{DG}[k], \Delta Q_{DG}[k], \Delta P_{HESS}[k], \Delta P_{grid}[k]\right) = \left(P_{DG}[0] + \Delta P_{DG}[k]\right)^2 + \left(Q_{DG}[0] + \Delta Q_{DG}[k]\right)^2 - 3V_{DG}[k]I_{rms-DG} \leq 0, \\ therefore \Rightarrow f \approx \left(\begin{array}{l} \left(\Delta P_{DG}[0], \Delta Q_{DG}[0], \Delta P_{ESS}[0], \Delta P_{grid}[0]\right) + \dfrac{\partial f}{\partial \Delta P_{DG}}\left(\Delta P_{DG}[k] - \Delta P_{DG}[0]\right) \\ + \dfrac{\partial f}{\partial \Delta Q_{DG}}\left(\Delta Q_{DG}[k] - \Delta Q_{DG}[0]\right) + \dfrac{\partial f}{\partial \Delta P_{HESS}}\left(\Delta P_{HESS}[k] - \Delta P_{HESS}[0]\right) \\ + \dfrac{\partial f}{\partial \Delta P_{grid}}\left(\Delta P_{grid}[k] - \Delta P_{grid}[0]\right) \end{array}\right) \end{array} \tag{48}$$

$$f(V,f)\left(\begin{array}{l} \left(\Delta P_{DG}[0], \Delta Q_{DG}[0], \Delta P_{ESS}[0], \Delta P_{grid}[0]\right) + \dfrac{\partial f}{\partial \Delta P_{DG}}\left(\Delta P_{DG}[k] - \Delta P_{DG}[0]\right) + \dfrac{\partial f}{\partial \Delta Q_{DG}}\left(\Delta Q_{DG}[k] - \Delta Q_{DG}[0]\right) \\ + \dfrac{\partial f}{\partial \Delta P_{HESS}}\left(\Delta P_{HESS}[k] + \Delta P_{HESS}[0]\right) + \dfrac{\partial f}{\partial \Delta P_{grid}}\left(\Delta P_{grid}[k] - \Delta P_{grid}[0]\right) + 1^T\theta[k] \\ 1^T\theta[k] \geq 0 \\ \theta[k] \geq 0 \\ \theta[k] \geq \dfrac{\partial f}{\partial P_{DG}}\left(\Delta P_{DG_i-\max}[k] - \Delta P_{DG_i-\min}[k]\right) \end{array}\right) \tag{49}$$

Table 4
Results of training based on INN structure

Observation	No. of samples	Mean square error
Training	87501	0.03599
Validation	18750	0.03658
Testing	18750	0.03711
Overall	125001	0.03656

Where w: is the disturbance vector, u: is the decision vector, $\widehat{w}$: is the prediction value of the uncertainty parameter, Δw_{upper}andΔw_{lower}: are the upper and lower limit of disturbance and prediction error,u_{lower}, u_{upper}: are the upper and lower limit of decision vector, μ: is the decision variables, θ_i: is the double variables.

2.2.1.3.2. Constraint Linearization. Because the constraints of the problem are nonlinear, the constraints of the problem are linearized using the Taylor expansion:

2.2.1.3.3. Transforming MPC-based Voltage and Frequency Regulation Model. This section describes the single-line optimization equation based on SDT:

$$\min\sum_{k=1}^{N_P}\left(\begin{array}{l}\|\widehat{V}_{critical}[k]-V_{ref}\|_{W_V}^2+\|SoC[k]-SoC(0)\|_{W_{SOC}}^2+\|\widehat{f}[k]-f_{ref}\|_{W_f}^2\\+\|\Delta Q_{DG}[k]-\Delta Q_{DG}[k-1]\|_{W_{Q-DG}}^2+\|\Delta P_{DG}[k]-\Delta P_{DG}[k-1]\|_{W_{P-DG}}^2\\+\|\Delta P_{HESS}[k]-\Delta P_{HESS}[k-1]\|_{W_{HESS}}^2+\|\Delta P_{Load}[k]-\Delta P_{Load}[k-1]\|_{W_{Load}}^2\\+\|\Delta P_{grid}[k]-\Delta P_{grid}[k-1]\|_{W_{grid}}^2\end{array}\right) \tag{50}$$

2.2.2. Voltage and frequency control model in secondary

2.2.2.1. Hypotheses.

1 The structure of the droop control specifies the distributed generation output voltage within the reference frame of the d-axis. V_{oq} is also considered equal to zero [35].

2 The continuous function $f(x):\mathrm{R}^n\Rightarrow\mathrm{R}^m$ can be approximated by the INN activation function. Therefore, due to the compact set $S\in\mathrm{R}^n$ and constant valuesδ_n, the hidden layers of the artificial neural network algorithm are equivalent to$f(x) = W^T\sigma(x)+\delta(x)$. Where $W\in\mathrm{R}^{l\times p}$ is the INN weight, $\delta(x)$is the INN approximation error, p is the INN output variables, l is the number of INN nodes. While the stated function is considered with the condition$\|\delta(x)\|<\delta_n, \forall x\in S$. As a result, the activation function in the INN algorithm is equivalent to:

$$\sigma_j(x) = \exp\left[\frac{-(x-\xi_j)^T*(x-\xi_j)}{v_j^2}\right], j = 1, 2, ..., l \tag{51}$$

Whereξ_j and v_j^2 is center and variance of the function considered, respectively [36-37].

1 3. For a compact setR^n, the ideal weights function of the INN are bounded by known positive values. Where $\|W\|_F\le W_\beta$ denotes the Frobenius norm [38].

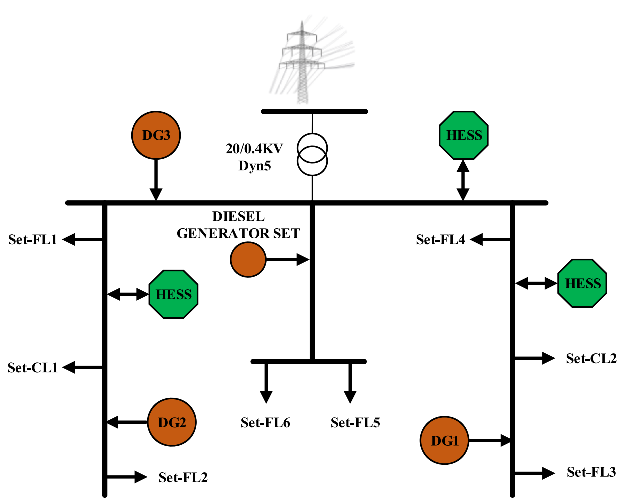

Fig. 5. Micro-grid model and its equipment

Table 5
Technical specifications of micro-grid

Nominal active power set required	1.5MW
Apparent power	1.7MVA
Nominal active power output generated by distributed generation sources	1.1MW
Power set HESS	0.44MW
Base power	1 MW=1pu
Power received from the main grid	0.4MW
Critical Load (CL)	0.4MW
Flexible Loads (FL)	1.1MW
Flexible load rate changes	0.1-0.4MW
Power of diesel generator (model SD500-GENERAC)	0.5MW
Micro-grid voltage	V_{LL}=400V, V_{ph}=220
Micro-grid frequency	50Hz
Line impedance per kilometer	Z=0.521+j0.083
Converter THD rate	THD<5%
Power factor	0.88≤ Cosφ ≤1
Upper limit SOC rate of HESS unit	90%
Low limit SOC rate of HESS unit	20%
Charging and discharging coefficient	0.95
Rate of power changes in normal and critical mode	0.1-0.4MW

2.2.2.2. Intelligent neural network structure model. The INN algorithm is used as an efficient regression tool to respond to computational complexity. Here, the structure and performance of the INN algorithm according to Fig. 4 is presented. First, before sending the training information to the neural network unit for regression analysis, the information is pre-processed. The task of information pre-processing is to minimize training data deviations to improve regression accuracy and computational efficiency. In this section, first the input and output data are expressed in terms of per-unit. Then, in another section, the existing information is normalized by the *min_max_scaler* conversion method. The normalized relationship is equal to:

$$\lambda_s^{new}(t) = \frac{\left(\lambda_s(t)-\min_s\lambda(t)\right)}{\left(\max_s\lambda(t)-\min_s\lambda(t)\right)} \tag{52}$$

Which s is an index of training data. $\min_s\lambda(t)$ and $\max_s\lambda(t)$ are the minimum and maximum characteristics of the voltage and frequency deviation factors in the total training data set. According to the normalization of Eq. (52), the data values are modeled based on binary data 0 and 1. The above information processing helps to create a regular search area for faster convergence of this algorithm. Eq. (53) is a model of the hidden layers of the INN algorithm:

$$y^l_{sk} = \sum_{j=1} x^l_{sj}\omega^l_{jk} + b^l_k \tag{53}$$

The output results are expressed in l_{th} of the hidden layer according to Eq. (53), where *s*: is the sample index, $y^l_{sk}$is the output data, *j* is the sample feature index, x^l_{sj}: is the input data, *k*: is the index of neurons, ω^l_{jk}: determined weight input j_{th} feature, b^l_k is the bias. The activation function model and other parameters are obtained according to the reference [39]. ω^l_{jk}andb^l_k are factors that must be calculated. Therefore, these two parameters are obtained based on the back-propagation algorithm. This method tries to guide the studied model to the optimal global value by changing the parameters of the neural network algorithm based on the gradient method [36-39]. Table 2 shows the summary of INN training structure, Table 3 describes the time calculations comparing INN and Monte Carlo methods and Table 4 shows the results of training based on INN structure

Next, the voltage and frequency control in the secondary part of the micro-grid based on Lyapunov stability theory is analyzed. In this control structure, the method of INN has been used in order to control the voltage and frequency deviation as well as the optimal distribution of active and reactive power.

2.2.2.3. Voltage control model based on INN. The relationship between the output and the input voltage variable based on the structure presented in the section (modeling of converters) is expressed. Therefore, by deriving Eq. (17) and substituting into relation (15), Eq. (54) is obtained and then the error tracking function ($Er_{tracking-1i}$) is expressed in Eq. (55). This error tracking variable is expressed to control the balanced distribution of reactive power:

$$\left(V''_{odi}\right) = \left(L_{fi}C_{fi}\right)^{-1}\left[\omega_i i_{lqi}L_{fi} - r_{fi}i_{ldi} - v_{odi} - (i'_{odi})L_{fi} + v_{idi}\right] \tag{54}$$

$$Er_{tracking-1i} = \left\{\sum_{j\in N_i} a_{ij}\left(n_{Qi}Q_i - n_{Qj}Q_j\right) + \sum_{j\in N_i} a_{ij}\left(v_{odi} - v_{odj}\right) + g_i\left(v_{odi} - v_{ref}\right)\right\} = (d_i + g_i)v_{odi} - \left\{\sum_{j\in N_i} a_{ij}\left(n_{Qi}Q_i - n_{Qj}Q_j\right) + \sum_{j\in N_i} a_{ij}v_{odi} + g_i v_{ref}\right\} \tag{55}$$

Since it is difficult to regulate the voltage between distributed generation sources by considering their reactive power based on droop factors, so the error function (55) is introduced to correct the distribution of power between distributed generation sources. As a result, by using the INN algorithm, an attempt is made to reduce this error ($v_{odi} - v_{ref}$). The next error variable is also expressed as Eq. (56):

$$Er_{tracking-2i} = (d_i + g_i)\left(v'_{odi}\right) - \phi_i \tag{56}$$

Where ϕ_i is the virtual control function expressed in Eq. (58). In order to control the voltage, the expansion of Lyapunov function is provided:

$$V_{1i} = \frac{1}{2}Er^2_{tracking1i} \Rightarrow^{\mathrm{Dif}\,V_{li}\mathrm{and substituting (53) and (54) into} (V'_{1i})} (V'_{1i}) = \left\{\begin{array}{l} Er_{tracking-1i}\left[(d_i + g_i)(v'_{odi})\right. \\ \left. -\left\{\sum_{j\in N_i} a_{ij}(v'_{odj}) + \sum_{j\in N_i} a_{ij}\left(n_{Qi}(Q'_j) - n_{Qj}(Q'_j)\right)\right\}\right] \end{array}\right\}$$
$$(V'_{1i}) = Er_{tracking-1i}\left[\left(Er_{tracking-2i} + \alpha_i\right) - \left\{\sum_{j\in N_i} a_{ij}(v'_{odi}) + \sum_{j\in N_i} a_{ij}\left(n_{Qi}(Q'_i) - n_{Qj}(Q'_j)\right)\right\}\right] \tag{57}$$

$$\left(\begin{array}{l} \phi_i = -k_{1i}e_{1i} + \left\{\sum_{j\in N_i} a_{ij}\left(v'_{odj}\right) - \sum_{j\in N_i} a_{ij}\left(n_{Qi}(Q'_i) - n_{Qj}(Q'_j)\right)\right\} \\ (Q'_i) = \omega_{icf}Q_i + \omega_{icf}\left(v_{oqi}i_{odi} - v_{odi}i_{oqi}\right) \end{array}\right) \Rightarrow (V'_{1i}) = Er_{tracking-1i}Er_{tracking-2i} - k_{1i}Er^2_{tracking-1i} \tag{58}$$

The following is another Lyapunov function:

According to the second hypothesis expressed in the secondary voltage control section, the INN structure and the controller model are expressed as Eq. (60).

$$v_{idi} = -Er_{tracking-1i} - k_{2i}Er_{tracking-2i} + F_i(x_i) \Rightarrow$$
$$F_i(x_i) = \left[\omega_i i_{lqi}L_{fi} + r_{fi}i_{ldi} - v_{odi} + (i'_{odi})L_{fi} - v_{idi} + \left(\frac{L_{fi}C_{fi}}{d_i + g_i}\right)(\phi'_i)\right] = W^{*T}_i\sigma_i(x_i) + \delta_i(x_i) \tag{60}$$

It should be noted that since the ideal neural network weight vector $W^{*T}_i \in \mathrm{R}^{1\times n}$ is an unknown value, its estimated value, which is equivalent to$\widehat{W}^T_i$, can be used to control the secondary voltage. *n* is also the number of nerve nodes. Therefore, neural network-based voltage control, weight estimation error, and its upgrade rules are:

$$\begin{array}{l} v_{idi} = -Er_{tracking-1i} - k_{2i}Er_{tracking-2i} - \widehat{W}^T_i\sigma_i(x_i) \\ therefore \Rightarrow \left(\widehat{W}'_i\right) = G_i\left(\sigma_i(x_i)Er_{tracking-2i} - k_i\|\,Er_{tracking-2i}\|\,\widehat{W}_i\right) \end{array} \tag{61}$$

Where $k_{1i}$and $k_{2i}$are positive constants and $G_i \in \mathrm{R}^{n\times n}$ is a diagonal matrices. Eq. (59) is expressed as Eq. (63) by substituting relations (60) and (61) in it. The input parameters of the INN algorithm based on voltage and its fluctuations as well as error tracking functions are also equal to the relation (62).

$$x_i = \left[v_{odi}, Er_{tracking-1i}, Er_{tracking-2i}, \left(v'_{odi}\right)\right] \tag{62}$$

$$\left(V'_{2i}\right) = \left(W^*_i - \widehat{W}_i\right)^T_i \sigma_i(x_i)Er_{tracking-2i} + \delta_i(x_i)Er_{tracking-2i} - k_{1i}Er^2_{tracking-1i} - k_{2i}Er^2_{tracking-2i} \tag{63}$$

2.2.2.4. Frequency control model based on INN. In this section, the micro-grid frequency control method based on the intelligent artificial

$$V_{2i}=V_{1i}+\frac{1}{2}\left(\frac{L_{fi}C_{fi}}{d_i+g_i}\right)Er^2_{tracking-2i}\overset{\text{Dif}}{\Rightarrow}(V'_{2i})=(V'_{1i})+Er_{tracking-2i}\left(\frac{L_{fi}C_{fi}}{d_i+g_i}\right)[(d_i+g_i)(v''_{odi})-(\phi'_i)]$$
$$\overset{\text{Substituting}(52)}{\Rightarrow}(V'_{2i})=Er_{tracking-1i}Er_{tracking-2i}-k_{1i}Er^2_{tracking-1i}+Er_{tracking-2i}\left[\omega_i i_{lqi}L_{fi}-r_{fi}i_{ldi}-v_{odi}-(i'_{odi})L_{fi}+v_{idi}-\left(\frac{L_{fi}C_{fi}}{d_i+g_i}\right)(\phi'_i)\right] \tag{59}$$

network algorithm is expressed by considering the proportionality of the active power distribution. In this section, the purpose is to synchronize the operating frequency based on the reference frequency. Derived from Eq. (14), Eq. (64) is obtained. By determining the error function of the INN algorithm based on Eq. (65), the Lyapunov V_{fi} function can be specified, which are:

$$(\omega'_i)=(\omega'_{ni})-m_{Pi}(P'_i) \tag{64}$$

$$Er_{tracking-\omega i}=(d_i+g_i)\omega_i+\sum_{j\in N_i}a_{ij}(m_{pi}P_i-{}_im_{pj}P_j)-\sum_{j\in N_i}a_{ij}\omega_j+g_i\omega_{ref} \tag{65}$$

Therefore, the controller input variable based on the frequency changes in Eq. (67) as well as the error weight function and dynamic changes based on the INN in order to control the frequency deviation in Eq. (68) can be expressed as follows:

$$(\omega'_{ni})=-k_{3i}Er_{tracking-\omega i}+(d_i+g_i)^{-1}*\left\{\sum_{j\in N_i}a_{ij}(\omega'_j)+\sum_{j\in N_i}a_{ij}(m_{pi}(P'_i)-m_{pj}(P'_j))\right\}+m_{pi}(P'_i) \tag{67}$$

$$W^*_{fi}\sigma_i(x_{fi})=m_{pi}(P'_i)+(d_i+g_i)^{-1}*\left\{\sum_{j\in N_i}a_{ij}\omega'_j+\sum_{j\in N_i}a_{ij}(m_{pi}(P'_i)-m_{pj}(P'_j))\right\}-\delta_i(x_{fi}) \tag{68}$$

Which by substituting Eqs. (67) and (68) in Eq. (66), the Lyapunov V_{fi} function is expressed as follows:

$$(V'_{fi})=\left(\delta_i(x_{fi})-k_{3i}+\widetilde{W}^T_{fi}\sigma_i(x_{fi})\right)Er_{tracking-\omega i} \tag{69}$$

$$(V'_{fi})=\frac{1}{2}(d_i+g_i)^{-1}Er^2_{tracking-\omega i}\overset{\text{Dif}}{\Rightarrow}(V'_{fi})=Er_{tracking-\omega i}(d_i+g_i)^{-1}(Er'_{tracking-\omega i})=Er_{tracking-\omega i}\left[(\omega'_i)-(d_i+g_i)^{-1}*\sum_{j\in N_i}a_{ij}(\omega'_j)+(d_i+g_i)^{-1}\sum_{j\in N_i}a_{ij}(m_{pi}(P'_i)-m_{pj}(P'_j))\right]$$
$$\overset{\text{Substituting}(62)}{\Rightarrow}(V'_{fi})=Er_{tracking-\omega i}\left[(\omega'_{ni})-m_{pi}(P'_i)-(d_i+g_i)^{-1}*\left\{\sum_{j\in N_i}a_{ij}(\omega'_j)+\sum_{j\in N_i}a_{ij}(m_{pi}(P'_i)-{}_im_{pj}(P'_j))\right\}\right] \tag{66}$$

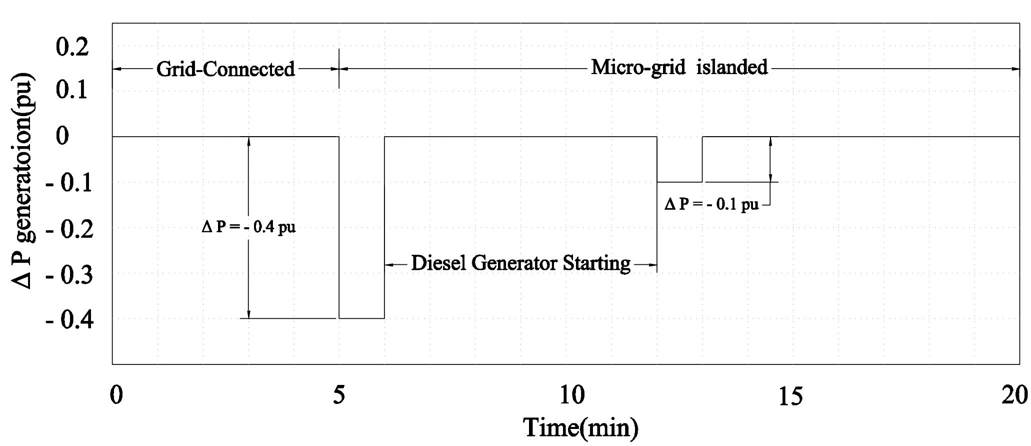

(a)

Fig 6. a) Island mode and critical fluctuations. b) Voltage control. c) Frequency control. d) Active power distribution dynamics related to distributed generation units and HESS. e) Reactive power distribution dynamics related to distributed generation units and HESS. f) SOC oscillations dynamics of HESS unit.

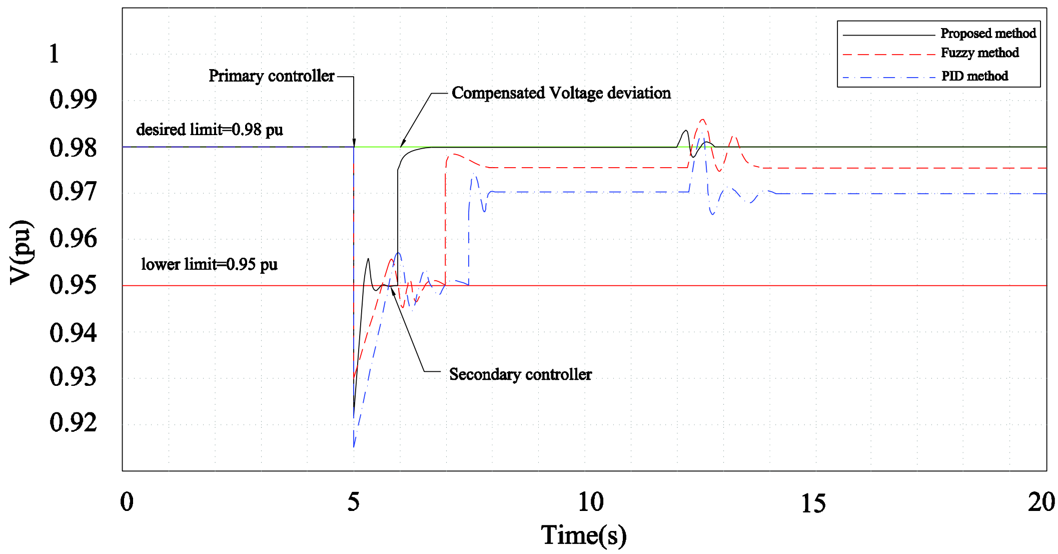

(b)

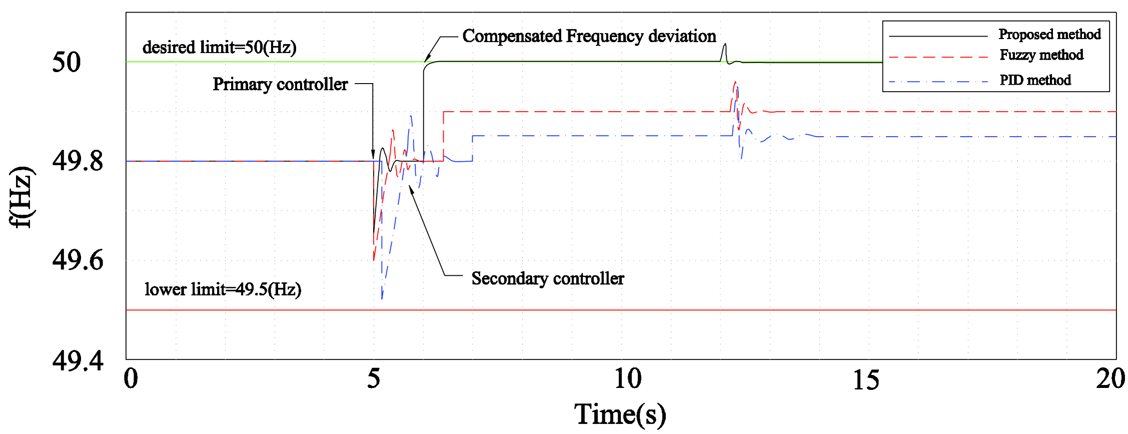

(c)

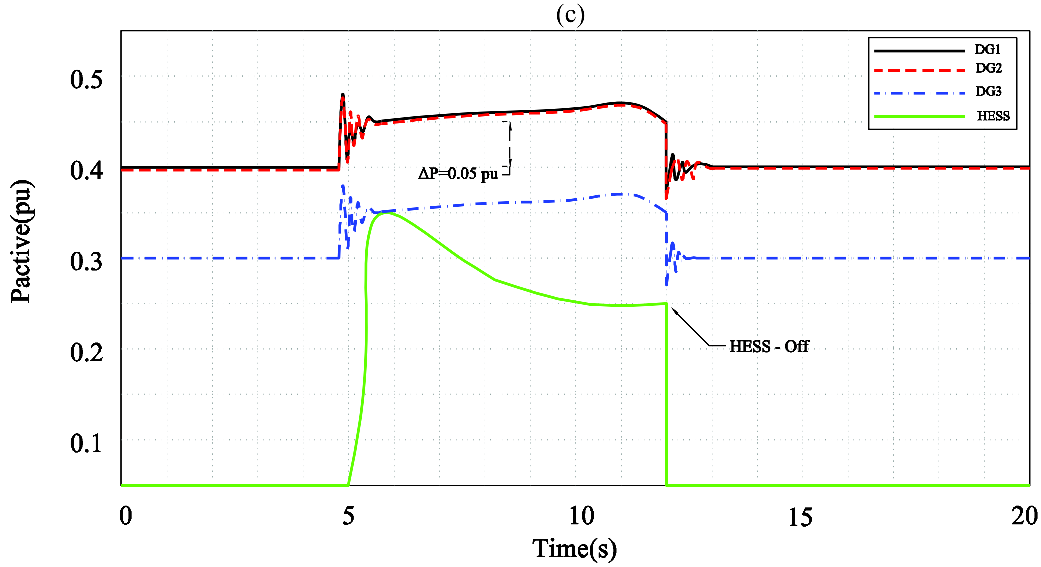

(d)

Fig 6. (*continued*).

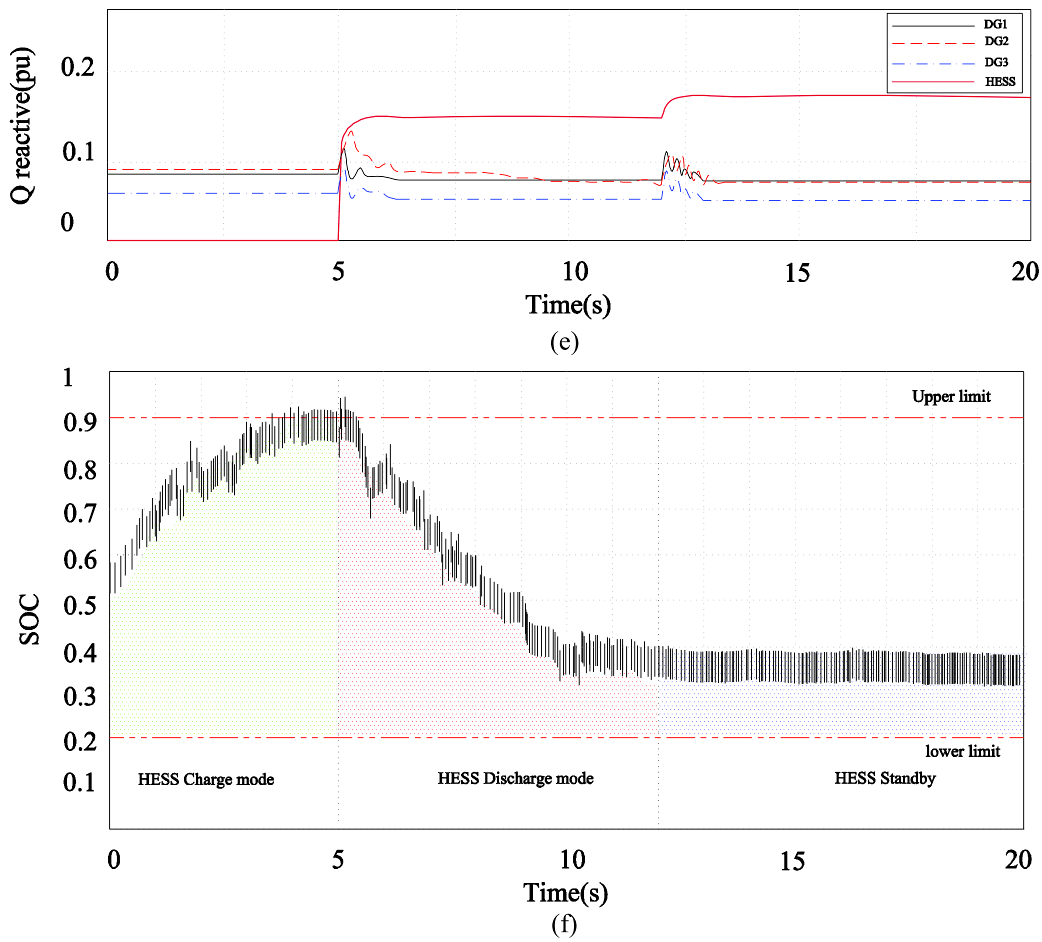

Fig 6. (*continued*).

As a result, frequency control at the secondary level based on the INN and according to the rules of updating as well as the error of its weight estimation function are:

$$(\omega'_{ni}) = -k_{3i}Er^2_{tracking-\omega i} - \widehat{W}^T_{fi}\sigma_i(x_{fi})Er_{tracking-\omega i} \tag{70}$$

$$\left(\widehat{W}'_{fi}\right) = R_i(\sigma_i(x_{fi})Er_{tracking-\omega i} - \rho_i\| Er_{tracking-\omega i}\| \widehat{W}_{fi}\right) \tag{71}$$

Which $k_{3i}$and $\rho_i$are a positive constant as well as $R_i \in \mathrm{R}^{n\times n}$ is positive diagonal matrix. INN input functions, which include changes in frequency, active power and error tracking functions, which are equal to:$x_{fi} = [v_{odi}, Er_{tracking-\omega i}, \omega_i, m_{pi}P_i]$.

3. Simulation and performance requirements

In this section, the requirements and execution algorithms in the simulation section are presented. Thus, as shown in Fig. 5, the network is considered part of the distribution network 20 / 0.4KV Rajaee Port in Iran. In order to standardize the existing network and use control protocols, changes have been made in the network to improve the performance of the proposed method. The technical specifications of micro-grid is presented in Table 5.

4. Results

4.1. Scenario 1: Voltage and frequency restoration based on micro-grid disconnection from main grid (load fluctuations)

Hypothesis:

- Diesel generator start-up time is between 5 to 8 minutes and distributed generation sources along with HESS unit are able to supply the loads in this time.
- The control method is examined in micro-grid number 1.
- The HESS has 55% of the initial charge.
- Disconnection and connection of power generation sources in minutes and the performance of controllers in seconds is considered.

At $t=5_s$, the micro-grid is disconnected from the main grid and continues to operate in island mode. In this scenario, the voltage and frequency control based on the proposed method and the use of HESS are investigated. The main grid delivers 0.4MW of power to the micro-grid. By disconnecting the injected power from the main grid, the micro-grid suffers from a severe power outage (critical power). Because the HESS power is available in a limited period of time (8 to 15 minutes), this equipment must operate in a coordinated manner and high sensitivity with the control method provided in the primary and secondary levels.

In order to be able to provide micro-grid power in longer time intervals, a 0.5MW diesel generator is considered as a backup unit (between 80 to 90% of the rated power is used). In this scenario, the basic factors of the micro-grid up to the start-up and connection of the backup diesel generator to the micro-grid are controlled by distributed generation units and HESS units. Fig. 6 examines the voltage, frequency, active and reactive power distributions, the voltage and frequency compensation structure, and the performance of the HESS unit. Fig (6-a) shows the uncertainty caused by the disconnection of the main grid. In this scenario, the proposed method is compared with two methods, fuzzy and PID controller. As can be seen in Fig (6-b, c), the proposed method restore the voltage and frequency in *t=5 to 5.5s* using the primary controller. In *t=5.5 to 6s*, the secondary controller is activated and by compensating the voltage and frequency deviation, it brings these two factors to the reference or predetermined values. The reference voltage is 0.98pu and the frequency is 50Hz. Fig (6-d, e, f) also show the distribution of active and reactive power of distributed generation sources as well as the active and reactive power of HESS units with their SOC, respectively. The HESS unit can control the reactive power distribution and instantaneous voltage fluctuations by using the super-capacitor feature and help to recover this factor. On the other hand, HESS unit is able to provide the required power of the micro-grid or store its excess power in order to control the voltage and frequency by using the high volume of the battery. It should also be noted that complete evacuation of HESS units in order to increase their lifespan is prevented. Accordingly, this equipment is operated between two levels of charge and discharge, which is 90% and 20% average. Comparison of the proposed method with other methods shows that this method has an acceptable performance against critical micro-grid fluctuations. The proposed method with high accuracy and speed, in addition to recovering voltage and frequency, also compensates for the deviation values from their reference.

4.2. *Scenario 2: Voltage and frequency restoration based on the uncertainty of load fluctuations in the state of sudden increase and decrease*

Hypotheses:

- The micro-grid is operated in island mode.
- Diesel generator is in operation mode.
- HESS is in full charge mode.
- Load uncertainty is based on sudden changes.
- The control method is examined in micro-grid 1.

In this scenario, the power consumption of the micro-grid is suddenly increased or decreased. Therefore, the proposed control structure at the primary and secondary levels is analyzed under these conditions. In

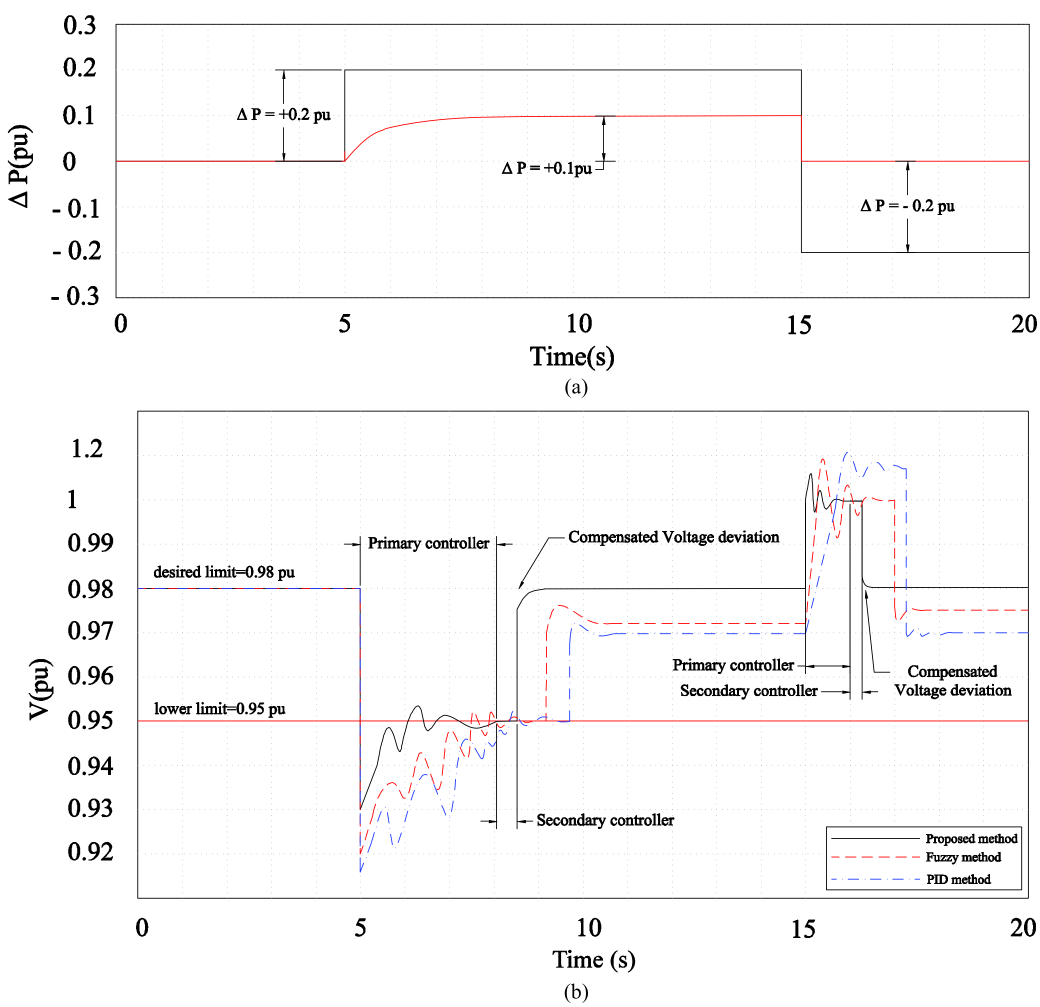

Fig. 7. **a)** Sudden load changes in island mode. **b)** Voltage control. **c)** Frequency control. **d)** Active power distribution dynamics related to distributed generation units and HESS. **e)** Reactive power distribution dynamics related to distributed generation units and HESS. **f)** SOC oscillations dynamics of HESS unit.

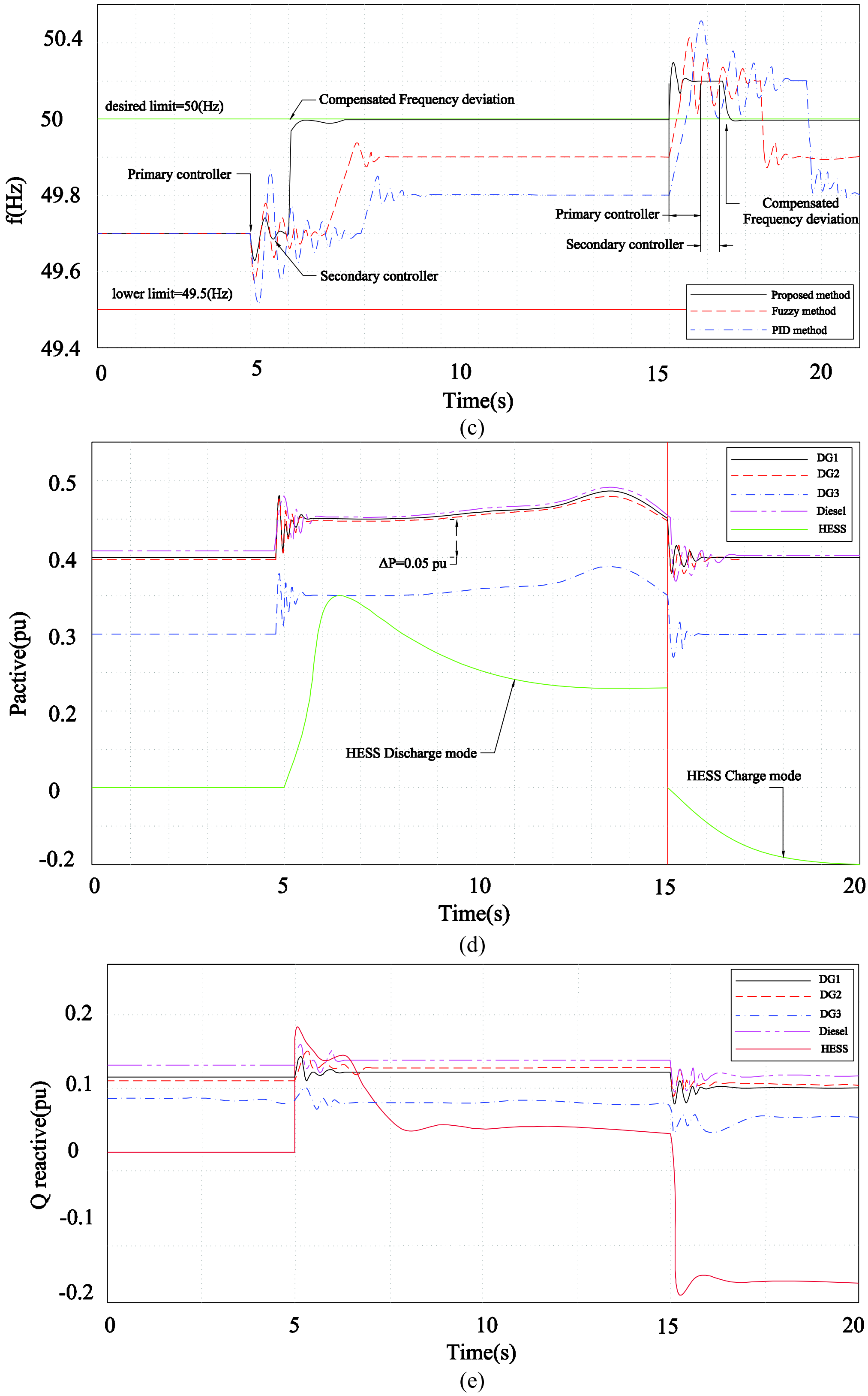

Fig. 7. (*continued*).

t=5s, the net power consumption of the micro-grid increases abruptly. This occurs due to uncertainty in the sudden increase in load (or even due to the outflow of power generation sources from the micro-grid). In this case, the combined controllers at the primary and secondary levels with proper coordination have the ability to control the fluctuations that have occurred. In the primary controller, by using the HESS structure and using the capabilities of the battery and super-capacitor, power fluctuations can be controlled by injecting active and reactive power.

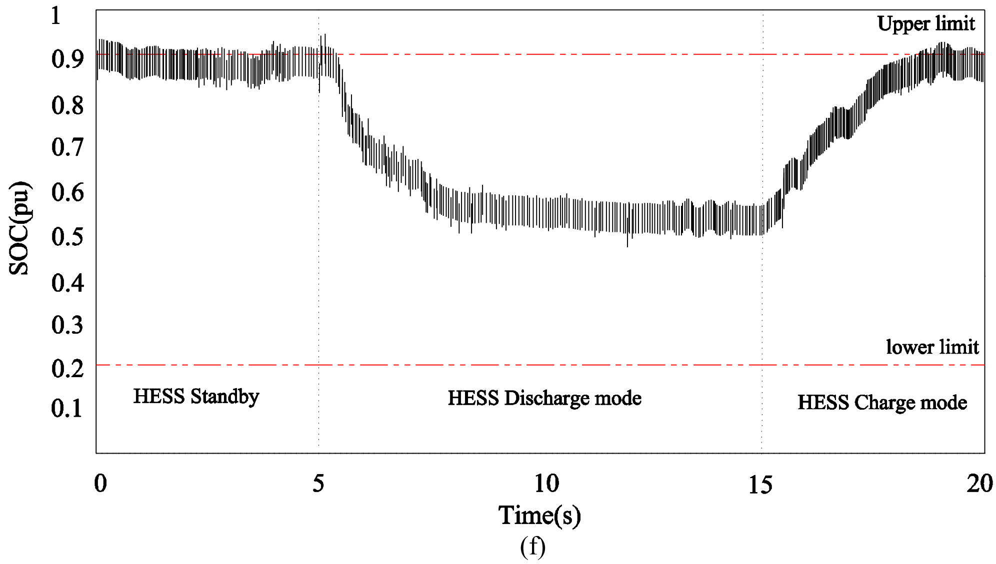

Fig. 7. (*continued*).

The use of backup diesel generators and HESS, in addition to recovering the voltage and frequency of the micro-grid in the primary, compensates their deviation from the reference in the secondary. Fig. 7 shows the control of voltage, frequency, active and reactive power distribution, and the operation of HESS in this scenario, respectively. As shown in Fig. (7-a), changes in active and reactive power have been investigated in the presence of a 100 KW induction motor and a 200 KW load. The induction motor requires a large amount of reactive power from the grid in a fraction of a second in addition to the active power. Exactly at the moment of connecting the motor to the micro-grid, the primary controllers can control the voltage and frequency fluctuations for a period of *t=5 to 8s* (motor starting), and then by increasing the motor power to the nominal value, the secondary controller is activated in *t=8.5s* to compensate for the deviation. In addition, distributed generation units of 0.05MW will be able to control the load.

In *t=15s*, 100KW induction motors and 400KW load are disconnected from the micro-grid, in which case the primary and secondary controllers maintain the voltage and frequency of the micro-grid at an acceptable level by activating HESS units (in order to store the excess micro-grid energy). In these conditions, as in the previous case, HESS play an important role. In this case, in order to control the voltage and frequency, the power injected into the micro-grid is stored by the HESS structure in coordination with the proposed methods. The coordination of HESS units and the proposed methods is of great importance and sensitivity. On the other hand, with the stabilization of the micro-grid after the oscillations, the diesel generator unit will be able to disconnect from the micro-grid. During this period, surplus power is stored by the HESS unit.

Therefore, in the stated conditions, the reason for using the prediction model based on uncertainty can be fully observed. The main reason for using the predictive model based on uncertainty factors in the primary is to provide a reliable control structure against instantaneous fluctuations of the micro-grid. Using the predictive model and considering the uncertainties, the proposed control method can be presented with higher coordination and reliability, along with the use of HESS structures and backup diesel generators. At the secondary, the proposed control method based on the accuracy of data with low tolerance has the ability to reduce the deviation from the reference of voltage and frequency factors. In the secondary, because the voltage and frequency control must be controlled in about a second, Fig. (7-b, f) shows that the method expressed in the secondary is capable of controlling sudden fluctuations well. In this figure, in addition to the proper coordination of the primary and secondary controllers, the coordination of the proposed method with the HESS and backup diesel generator supports the appropriate dynamic behavior of these two units.

4.3. *Scenario 3: Voltage and frequency restoration based on DG uncertainty and load step fluctuation*

Hypothesis:

- Flexible loads are cut-down in three 0.1MW stages.
- The micro-grid is in island mode and the backup diesel generator is in operation mode.
- HESS is in full charge mode.
- The control method is examined in micro-grid 1.

In this scenario, part of the net grid power is reduced by removing one of the distributed generation sources (0.3 MW). In this scenario, the operation algorithm is presented in two parallel parts. As shown in Fig. 8 in the first section, voltage and frequency fluctuations resulting from DG interruption are controlled by HESS, backup diesel generator, primary, secondary controllers. In the second part, considering that the net production capacity of the micro-grid is reduced and also the HESS are decreasing, then power management on flexible loads is presented. Under these conditions, flexible loads are removed from the grid by reducing the 0.1 MW steps in three steps to prevent the voltage and frequency fluctuations (Fig (8-b)). At *t=5s*, the DG_3 unit shuts down. Therefore, in the first step and in *t=5s*, a load equal to 100 KW is cut off. Load reductions continue at *t=6s* and *t=7s*. In this scenario, the allowable fluctuation of the micro-grid frequency equal to 0.5 Hz and the allowable voltage fluctuation of 5% is considered.

At *t=5s* after the DG_3 is disconnected, the HESS are activated to manage the reduced power compensation. In this scenario, in order to create critical conditions, the net power of the HESS unit is considered equivalent to critical and sensitive loads. In this case, the HESS units first control the voltage and frequency fluctuations according to the primary controller. Then, the secondary controller based on the INN algorithm, compensates for the deviation by controlling the power distribution of the HESS units and reducing the power of the flexible loads. As shown in Fig. (8-d), when the micro-grid frequency is reduced to 49.7Hz, then a power equivalent to 100 KW is cut off from the flexible loads. Then again, by reducing the frequency to 49.6Hz, the power equivalent to 100 KW of flexible loads is reduced. Here the critical frequency is 49.5Hz. 0.1 Hz is considered as a safety margin in frequency control. Fig (8-b,e) shows how the proposed method works compared to other methods. At

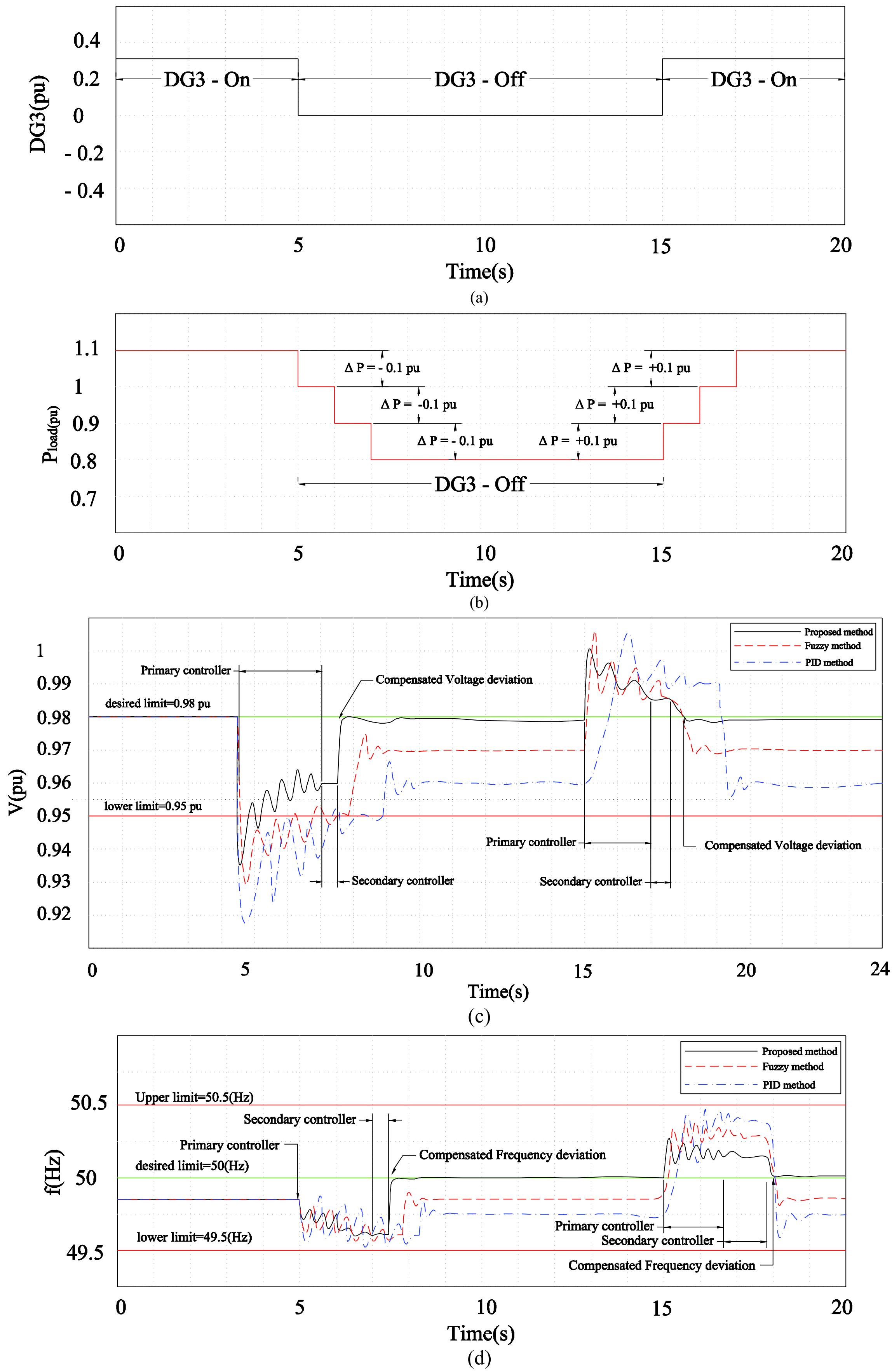

Fig. 8. **a)** Disconnect the DG3 unit. **b)** Flexible load management. **c)** Voltage control. **d)** Frequency control. **e)** SOC oscillation dynamics of HESS unit

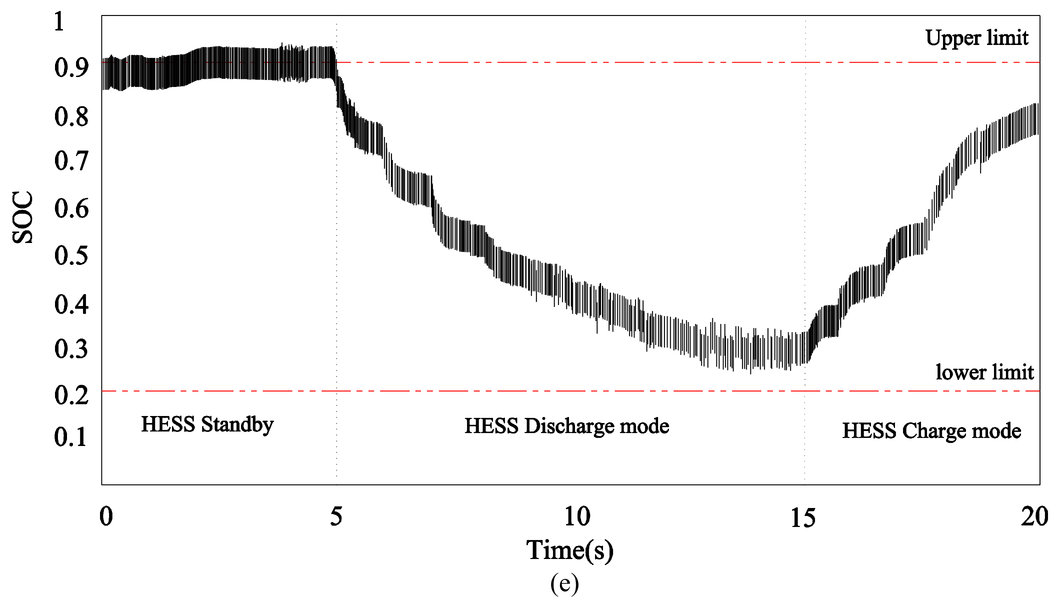

(e)

Fig. 8. (*continued*).

t=15s, the DG_3 is reconnected to the micro-grid. In this case, due to the prevention of severe fluctuations and also the recovery of the HESS unit power, the flexible loads in 0.1MW steps are connected to the micro-grid. These management conditions ensure the stability of the micro-grid after disturbances occur. The Flexible load management will also improve the voltage profile and micro-grid frequency. With the proper distribution of active and reactive powers as well as the coordinated performance of HESS units with the control method are presented, the voltage and frequency factors are also controlled in this scenario with high accuracy and speed.

4.4. Scenario 4: Voltage and frequency restoration considering the effect of communication delay

One of the most important and indispensable parameters in proposing control methods is the delay caused by communication infrastructure. Because the proposed methods are used in milliseconds and seconds, then communication latency becomes significantly more important. If this delay is not taken into account in modeling the control method, then the accuracy of the proposed method will be unreliable. In this scenario, the effect of communication delay on the proposed control method is presented. Communication infrastructure latency is considered in the range of 200ms and 400ms. In this case, the proposed control method (Fig (9-b, c)) is examined and compared with Fuzzy method (Fig (9-d, e)). The disturbances considered in this scenario are equivalent to disconnecting or reconnecting a load of 0.2MW. If the communication infrastructure latency increases, then the instability and fluctuations of the micro-grid will increase sharply. The result of this comparison shows that the proposed method has an acceptable response compared to other methods. The proposed method shows higher speed and accuracy than other methods in controlling fluctuations and deviations of voltage and frequency factors.

Therefore, the proposed model by controlling voltage and frequency fluctuations in a shorter period of time prevents the micro-grid to lead to instability and protects the micro-grid against instability. This point is important because by combining the predictive method and the INN algorithm, several important features have been considered in the proposed method. In order to express the importance of speed and high accuracy of the proposed method, it should be stated that if communication infrastructure delays and sudden load changes in the critical state are considered, coordination between grid control equipment will not be possible and micro-grids will face instability and collapse. As a result, by creating a suitable context and using the features of the proposed method; optimal control of essential micro-grid parameters can be suggested. Important features of the proposed control method are:

- First feature: accurate prediction of micro-grid errors and uncertainties makes it easier to control micro-grid fluctuations and deviations (primary level).
- The second feature is memory and learning in the INN method, which makes it easier to deal with micro-grid errors (secondary level).
- And speed, which is the third characteristic due to the combination of these two methods. The speed of dealing with micro-grid fluctuations is important because the proposed method can respond to fluctuations in the shortest possible time. At the same time, the shorter the response time, the more reliable the micro-grid stability can be achieved.

4.5. Real time monitoring/control hardware, experimental Set-Up and validation results

In this section, the rapid control prototyping (RCP) of micro-grid control based on software and hardware infrastructure is provided. The software infrastructure used is based on MATLAB/Simulink and RT-LAB software. Important and basic hardware infrastructure is also based on the use of OPAL-RT hardware (OP5600 and OP8660) and LabVolt Electromechanical Training System. Accordingly, Fig. 10 shows the relationship between the simulation environment and the hardware environment (experimental set-up). The proposed control system based on real time structures is analyzed and operated, which requires the use of two equipment, OP5600 and OP8660. RT-LAB is the real-time technology that is revolutionizing the way model-based design is performed. Through its openness, it has the flexibility to be applied to any simulation and control problem, and its scalability provides a low-risk entry point for any application, allowing the developer to add compute power where and when needed–whether it is to speed up simulations or for real-time hardware in the loop applications. RT-LAB provides tools for running and monitoring the simulations or controls on various runtime targets. An open architecture enables RT-LAB to work with MATLAB/Simulink.

The OP5600 as a real-time digital simulator consists of two primary

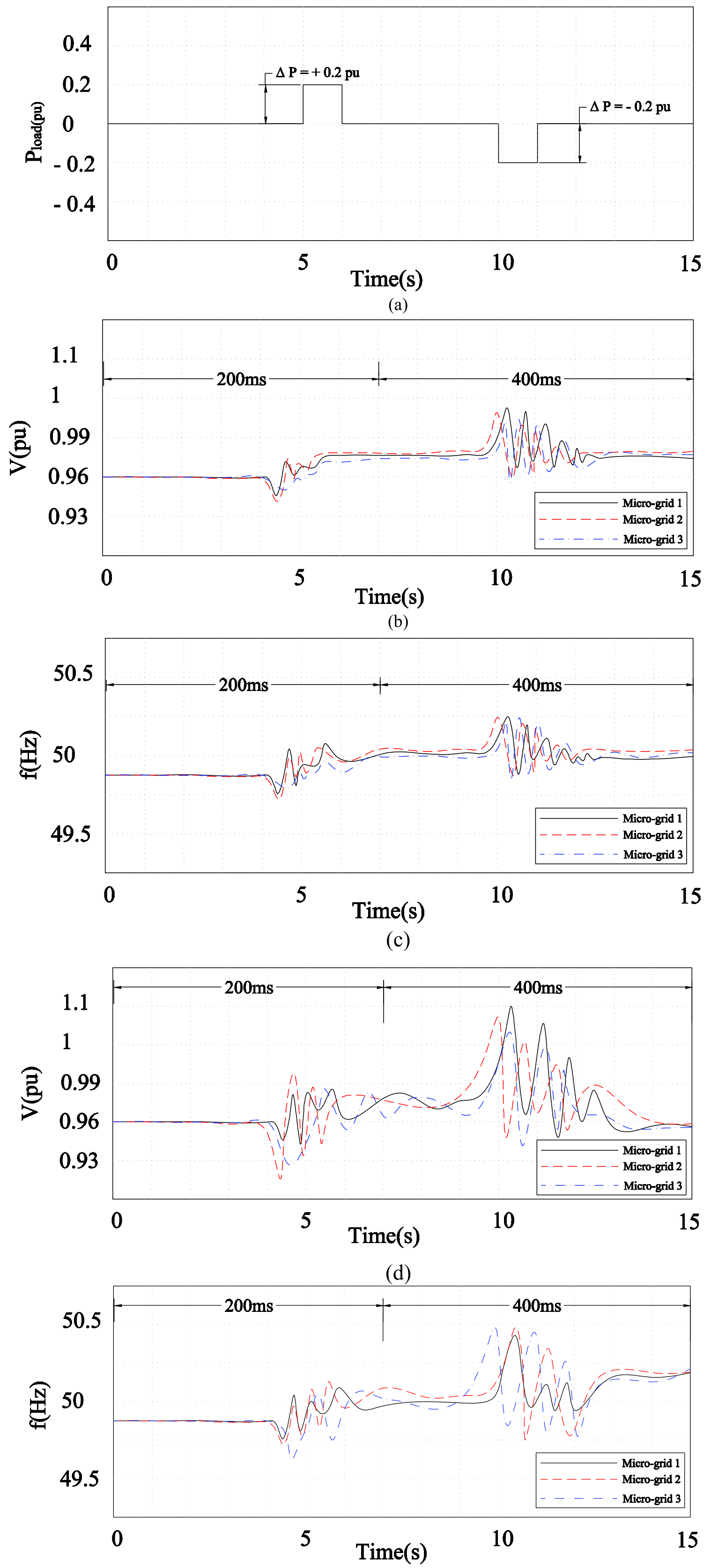

Fig. 9. a) Load fluctuations. **b)** Voltage control by the proposed method in microgrids and in different zones. **c)** Frequency control by the proposed method in microgrids and in different zones **d)** Voltage control by Fuzzy method in microgrids and in different zones. **e)** Frequency control by Fuzzy method in microgrids and in different zones.

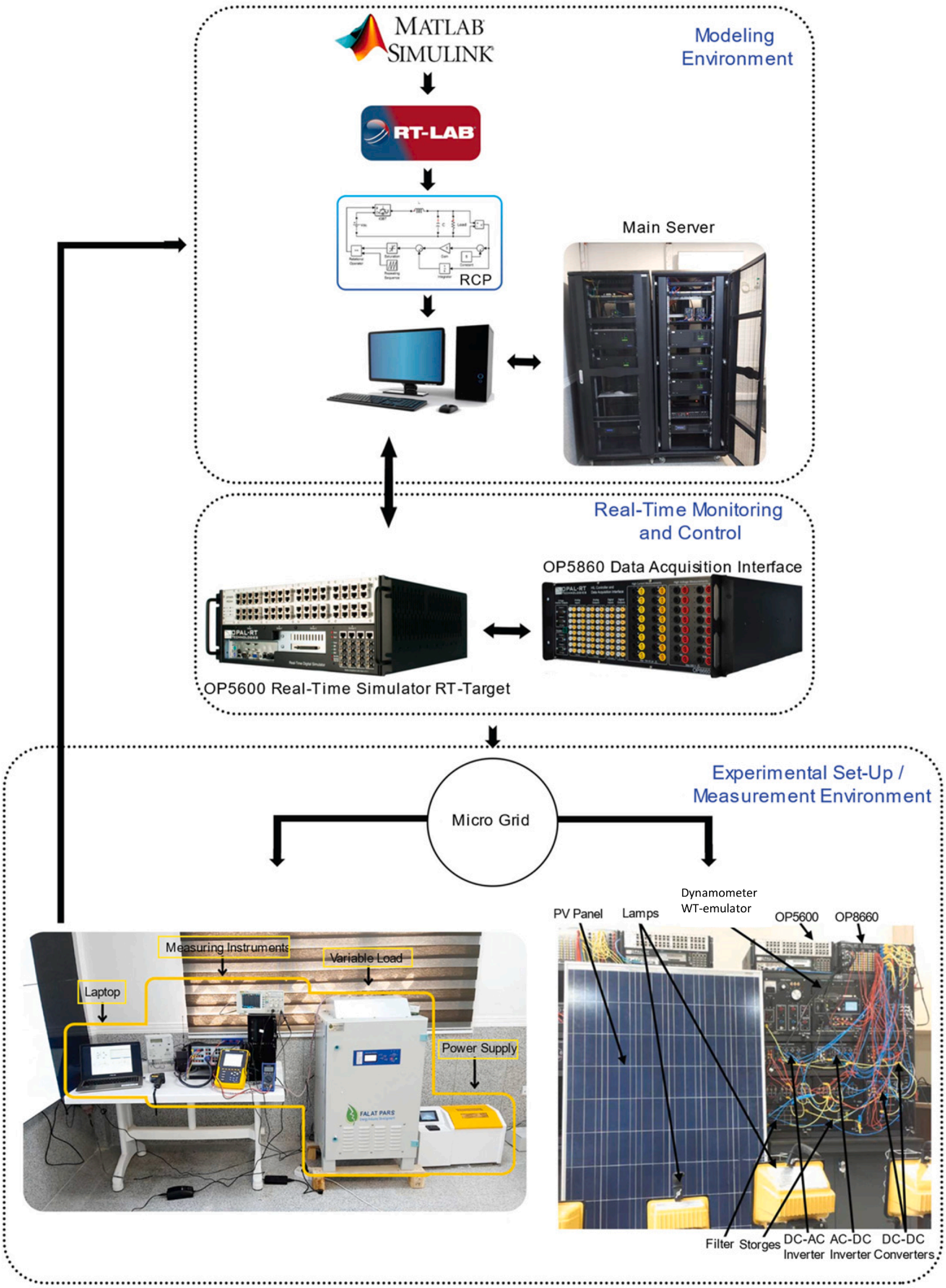

Fig. 10. Real Time Monitoring, Control Hardware and Experimental Set-Up.

and secondary parts. The primary part includes analog and digital input and output modules (I/O). The secondary part includes the multi-core processor computer and FPGA capable of running the entire OPAL-RT suite of real-time simulation software. This equipment provides a good platform for achieving the best accuracy, based on the real-time RCP structure to control critical micro-grid factors. Therefore, this equipment is considered as a powerful tool for RCP and hardware-in-the-loop (HIL). The technical specifications of this equipment are presented in Table 6.

Table 6
The OP5600 specifications

CPU	1x Xeon Gold 5222 (4 cores - 3.80 GHz)
FPGA	Xilinx® Artix®-7 FPGA, 200T
Software Platform Compatibility	RT-LAB and HYPERSIM
High speed communications	4x SFP socket, 1 to 5Gbps, duplex multi-mode optical fiber (50/125 or 65/125μm), Xilinx Aurora compatible Up to 5 PCI or PCIe interface cards
I/O boards (8 slots per system)	Analog - 16 channels per slot (max. of 128 per system)
	Digital - 32 channels per slot (max. of 256 per system)
I/O monitoring	Mini-BNC for up to 16 Analog/Digital channels
Connectivity	Ethernet, RS-232, VGA, Keyboard and mouse
Dimensions (HxWxD) & weight	17.8 × 47.7 × 49.3 cm, Simulator: 9.07 - 15 Kg

The OP8660 is an HIL Controller and data acquisition interface designed to be used with the complete OP5600 simulation system to provide a supplementary signal conditioning. It contains high current and high voltage input conditioning modules, which allow conversion of current and voltage to $\pm$10V voltage signals. The OP8660 creates a suitable connection between the software environment (the real-time simulator OP5600 based on MATLAB/Simulink) and the hardware (micro-grid system: renewable and non- renewable energy resource, storages, power electronics, variable load ...). All measurement frameworks; Testing and control is designed in MATLAB / Simulink software environment and then integrated with RT-LAB for real time monitoring. RT-LAB is also a real-time software environment capable of running real-time RCP based on OPAL-RT hardware (OP5600 and OP8660). The model designed in MATLAB / Simulink environment is loaded on RT-LAB software environment. The programmed commands are then loaded on OP5600 and OP8660 by this software environment. Finally, all management signals are sent to the micro-grid.

As shown in Fig. 10, the proposed model is programmed based on both software and hardware environments. According to Fig. 10, the simulation and experimental environment is divided into the following three parts.

1 Modeling Environment (MATLAB / Simulink software, RT-LAB software environment, Main Server and Personal Computer).
2 Real Time Monitoring and Control (OPAL-RT hardware (OP5600 and OP8660)).
3 Experimental Set-Up and Measurement Environment (Control Hardware and Experimental Set-Up).

The modeling environment includes MATLAB / Simulink and RT-LAB software along with hardware equipment to run the proposed models. Real Time monitoring and control includes OPAL-RT hardware (OP5600 and OP8660). In the experimental set-up section, two basic sections are presented. The first part is the micro-grid laboratory model and the second part is the measurement, sampling and monitoring environment, which is directly related to the user software environment. Therefore, the results are provided to the micro-grid control and management unit in the form of feedback signals. The INN calculation and the proposed method are implemented on MATLAB / Simulink software R2019b, and the hardware environment is a laptop with Intel®Core™ i7-7600U 2.8 GHz CPU, and 16.00 GB RAM. Here, for validation, the simulation and experimental results are compared. Therefore, the experimental and simulation results of Scenario 4 (voltage and frequency control of micro-grid No. 1) are presented in Fig. 11.

As shown in Fig. 11, the tolerance of simulation and experimental results is between 2 and 5%. This error also depends on various reasons such as laboratory conditions, quality of sampling and measurement equipment. Due to the fact that measurement and sampling equipment are classified in different classifications based on measurement error, so the simulation results and experimental results can be seen with a tolerance range of 2 to 5%. Therefore, in general, the tolerance observed in the experimental results compared to the simulation results is acceptable. Because this tolerance does not affect the performance of the results of the proposed model and the proposed model is used with appropriate accuracy.

5. Conclusion

In this paper, an intelligent method based on MPC and INN algorithm to control the voltage and frequency at the primary and secondary control levels is described. Accordingly, the voltage and frequency control at the primary is considered by the MPC based on the uncertainties of power generation sources and load fluctuations. At the primary level, the voltage and frequency control model is presented as a multi-objective optimization problem in a multi-time period according to the effective parameters. In addition to linearization, this model has become a quadratic equation. Secondly, using the INN model, the deviation from the voltage and frequency reference is compensated by using the error tracking function. In this section, compensation for deviation from the reference is based on the use of Lyapunov stability function and error tracking function. The HESS unit and the backup diesel generator have been used as two practical tools to advance the objectives of this research. In order to validate, the simulation results were compared with Fuzzy methods and PID controller. According to the obtained results, the proposed method has features such as high speed in error detection, high speed in responding to fluctuations and disturbances of micro-grids, increasing accuracy in reducing deviations from the reference values of voltage and frequency, providing intelligent management of power and energy distribution between production sources and HESS as well as two characteristics of prediction and learning that are achieved by combining the model of predictive control and neural network. These two features have increased the reliability factor of using the proposed method. Finally, in order to evaluate the performance of the proposed method, the experimental results based on the electrical distribution network of Rajaee Port in Iran have been analyzed.

Authorship Statement

All persons who meet authorship criteria are listed as authors, and all authors certify that they have participated sufficiently in the work to take public responsibility for the content, including participation in the concept, design, analysis, writing, or revision of the manuscript. Furthermore, each author certifies that this material or similar material has not been and will not be submitted to or published in any other publication before its appearance in the Journal of '***Electric Power Systems Research***'.

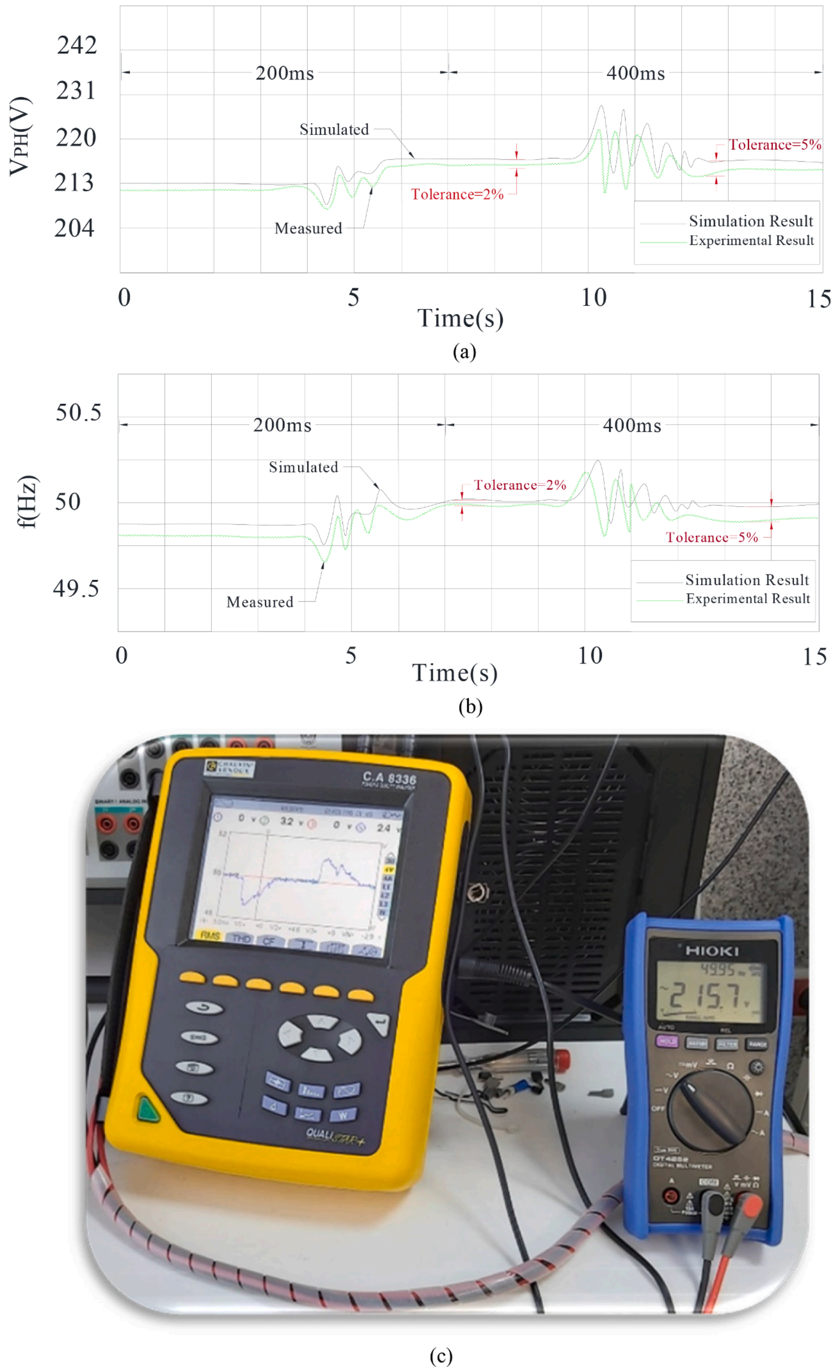

Fig. 11. Comparison of experimental and simulated results in Scenario 4. **a)** Voltage control based on the proposed method. **b)** Frequency control based on the proposed method. **c)** Experimental results of frequency control.

CRediT authorship contribution statement

Reza Sepehrzad: Conceptualization, Methodology, Software, Investigation, Validation, Writing – original draft, Formal analysis. **Amirhossein Mahmoodi:** Writing – review & editing, Software, Formal analysis. **Seyedeh Yosra Ghalebi:** Writing – review & editing, Visualization, Investigation, Formal analysis. **Ali Reza Moridi:** Software, Investigation, Writing – review & editing. **Ali Reza Seifi:** Supervision, Project administration, Investigation, Conceptualization, Methodology.

Declaration of competing interest

The authors declare that they have no known competing financial interests or personal relationships that could have appeared to influence the work reported in this paper.

Reference

[1] C.N. Papadimitriou, E.I. Zountouridou, N.D. Hatziargyriou, Review of hierarchical control in DC microgrids, Electric Power Syst. Res. 122 (2015) 159–167.
[2] N. Hatziargyriou, H. Asano, R. Iravani, C. Marnay, Micro-grids, IEEE Power Energy Mag 5 (4) (2007).
[3] Ahmed Saad, Tarek Youssef, Ahmed T. Elsayed, Amr Amin, Omar Hanafy Abdalla, Osama Mohammed, Data-centric hierarchical distributed model predictive control for smart grid energy management, IEEE Trans. Ind. Inf. 15 (7) (2018) 4086–4098.
[4] Abel Antonio-Ferreira, Carlos Collados-Rodriguez, Oriol Gomis-Bellmunt, Modulation techniques applied to medium voltage modular multilevel converters

for renewable energy integration: a review, Electric Power Syst. Res. 155 (2018) 21–39.

[5] Dana-Alexandra Ciupageanu, Linda Barelli, Gheorghe Lazaroiu, Real-time stochastic power management strategies in hybrid renewable energy systems: a review of key applications and perspectives, Electric Power Syst. Res. 187 (2020), 106497.

[6] Frate, Guido Francesco, Lorenzo Ferrari, and Umberto Desideri. "Energy storage for grid-scale applications: Technology review and economic feasibility analysis." Renewable Energy (2020).

[7] Reza Govahian Jahromi, Ali Reza Seifi, The demand side management program considering AC/DC hybrid distribution system concept based on the energy hub. 2016 24th Iranian Conference on Electrical Engineering (ICEE), IEEE, 2016, pp. 384–388.

[8] Reza Sepehrzad, Mohammad Esmaeil Hassanzadeh, Ali Reza Seifi, Mahnaz Mazinani, An efficient multilevel interconnect control algorithm in AC/DC micro-grids using hybrid energy storage system, Electric Power Syst. Res. 191 (2021), 106869.

[9] Mateo Beus, Frederik Banis, Hrvoje Pandžić, Niels Kjølstad Poulsen, Three-level hierarchical microgrid control—model development and laboratory implementation, Electric Power Syst. Res. 189 (2020), 106758.

[10] M. Jayachandran, G. Ravi, Decentralized model predictive hierarchical control strategy for islanded AC microgrids, Electric Power Syst. Res. 170 (2019) 92–100.

[11] Sepehrzad, Reza, Ali Reza Moridi, Mohammad Esmaeil Hassanzadeh, and Ali Reza Seifi. "Intelligent energy management and multi-objective power distribution control in hybrid micro-grids based on the advanced fuzzy-PSO method." ISA Trans. (2020).

[12] Fermín Rodríguez, Ane M. Florez-Tapia, Luis Fontán, Ainhoa Galarza, Very short-term wind power density forecasting through artificial neural networks for microgrid control, Renew. Energy 145 (2020) 1517–1527.

[13] Thomas John, So Ping Lam, Voltage and frequency control during microgrid islanding in a multi-area multi-microgrid system, IET Generat. Trans. Distribut. 11 (6) (2017) 1502–1512.

[14] Stefano Leonori, Alessio Martino, Fabio Massimo Frattale Mascioli, Antonello Rizzi, Microgrid energy management systems design by computational intelligence techniques, Appl. Energy 277 (2020), 115524.

[15] Hassan Bevrani, Shoresh Shokoohi, An intelligent droop control for simultaneous voltage and frequency regulation in islanded microgrids, IEEE Trans. Smart Grid 4 (3) (2013) 1505–1513.

[16] Ramon Blasco-Gimenez, Salvador Ano-Villalba, Johel Rodríguez-D'Derlée, Francisco Morant, Soledad Bernal-Perez, Distributed voltage and frequency control of offshore wind farms connected with a diode-based HVdc link, IEEE Trans. Power Electron. 25 (12) (2010) 3095–3105.

[17] Junyan Hu, Parijat Bhowmick, A consensus-based robust secondary voltage and frequency control scheme for islanded microgrids, Int. J. Electr. Power Energy Syst. 116 (2020), 105575.

[18] Yinliang Xu, Hongbin Sun, Wei Gu, Yan Xu, Zhengshuo Li, Optimal distributed control for secondary frequency and voltage regulation in an islanded microgrid, IEEE Trans. Ind. Inf. 15 (1) (2018) 225–235.

[19] Ramon Zamora, Anurag K. Srivastava, Multi-layer architecture for voltage and frequency control in networked microgrids, IEEE Trans. Smart Grid 9 (3) (2016) 2076–2085.

[20] Hongxun Hui, Yi Ding, Yonghua Song, Saifur Rahman, Modeling and control of flexible loads for frequency regulation services considering compensation of communication latency and detection error, Appl. Energy 250 (2019) 161–174.

[21] Yifei Guo, Qiuwei Wu, Houlei Gao, Xinyu Chen, Jacob Østergaard, Huanhai Xin, MPC-based coordinated voltage regulation for distribution networks with distributed generation and energy storage system, IEEE Trans. Sustain. Energy 10 (4) (2018) 1731–1739.

[22] Dimitris Bertsimas, Melvyn Sim, The price of robustness, Oper. Res. 52 (1) (2004) 35–53.

[23] Bing Yan, Marialaura Di Somma, Giorgio Graditi, Peter B. Luh, Markovian-based stochastic operation optimization of multiple distributed energy systems with renewables in a local energy community, Electric Power Syst. Res. 186 (2020), 106364.

[24] M. Eslahi, A.Foroughi Nematollahi, B. Vahidi, Day-Ahead scheduling of centralized energy storage system in electrical networks by proposed stochastic MILP-Based bi-objective optimization approach, Electric Power Syst. Res. 192 (2021), 106915.

[25] Ayse Selin Kocaman, Emin Ozyoruk, Shantanu Taneja, Vijay Modi, A stochastic framework to evaluate the impact of agricultural load flexibility on the sizing of renewable energy systems, Renew. Energy 152 (2020) 1067–1078.

[26] Zhiwei Xu, Duncan S. Callaway, Zechun Hu, Yonghua Song, Hierarchical coordination of heterogeneous flexible loads, IEEE Trans. Power Syst. 31 (6) (2016) 4206–4216.

[27] Ray Daniel Zimmerman, Carlos Edmundo Murillo-Sánchez, Robert John Thomas, MATPOWER: Steady-state operations, planning, and analysis tools for power systems research and education, IEEE Trans. Power Syst. 26 (1) (2010) 12–19.

[28] Nagaraju Pogaku, Milan Prodanovic, Timothy C. Green, Modeling, analysis and testing of autonomous operation of an inverter-based microgrid, IEEE Trans. Power Electron. 22 (2) (2007) 613–625.

[29] Vahidreza Nasirian, Seyedali Moayedi, Ali Davoudi, Frank L. Lewis, Distributed cooperative control of DC microgrids, IEEE Trans. Power Electron. 30 (4) (2014) 2288–2303.

[30] Eduardo F. Camacho, Carlos Bordons Alba, Model Predictive Control, Springer Science & Business Media, 2013.

[31] M. Khalid, Andrey V. Savkin, An optimal operation of wind energy storage system for frequency control based on model predictive control, Renew. Energy 48 (2012) 127–132.

[32] Roozbeh Sangi, Dirk Müller, A novel hybrid agent-based model predictive control for advanced building energy systems, Energy Convers. Manage. 178 (2018) 415–427.

[33] Yao Li, Liying Li, Chao Peng, Jianxiao Zou, An MPC based optimized control approach for EV-based voltage regulation in distribution grid, Electric Power Syst. Res. 172 (2019) 152–160.

[34] Motakuri V. Ramana, Levent Tunçel, Henry Wolkowicz, Strong duality for semidefinite programming, SIAM J. Optim. 7 (3) (1997) 641–662.

[35] Xiangyu Wu, Chen Shen, Reza Iravani, A distributed, cooperative frequency and voltage control for microgrids, IEEE Trans. Smart Grid 9 (4) (2016) 2764–2776.

[36] Wei He, David Ofosu Amoateng, Chenguang Yang, Dawei Gong, Adaptive neural network control of a robotic manipulator with unknown backlash-like hysteresis, IET Control Theory Appl. 11 (4) (2016) 567–575.

[37] Young Ho Kim, Frank L. Lewis, Output feedback control of rigid robots using dynamic neural networks. Proceedings of IEEE International Conference on Robotics and Automation, vol. 2, IEEE, 1996, pp. 1923–1928.

[38] Frank L. Lewis, Aydin Yesildirek, Kai Liu, Multilayer neural-net robot controller with guaranteed tracking performance, IEEE Trans. Neural Netw. 7 (2) (1996) 388–399.

[39] Michael A. Nielsen, Neural Networks and Deep Learning. Vol. 2018, Determination press, San Francisco, CA, 2015.